JOURNAL OF GEOPHYSICAL RESEARCH, VOL. 99, NO. B6, PAGES 12,191–12,209, JUNE 10, 1994

Escarpment evolution on high-elevation rifted margins: Insights derived from a surface processes model that combines diffusion, advection, and reaction

Henk Kooi and Christopher Beaumont
Department of Oceanography, Dalhousie University, Halifax, Nova Scotia, Canada

Abstract. Experiments with a surface processes model of large-scale (1-1000 km) long-term (1-100 m.y.) erosional denudation are used to establish the controls on the evolution of a model escarpment that is related to the rifting of a continent. The model describes changes in topographic form as a result of simultaneous short- and long-range mass transport representing hillslope (diffusive) processes and fluvial transport (advection), respectively. Fluvial entrainment is modeled as a first-order kinetic reaction which reflects the erodibility of the substrate, and therefore the fluvial system is not necessarily carrying at capacity. One-dimensional and planform models demonstrate that the principal controls on the evolution of an initially steep model escarpment are (1) antecedent topography/drainage; (2) the timescale (or equivalently a length scale) in the fluvial entrainment reaction; (3) the flexural response of the lithosphere to denudation; and (4) the relative efficiencies of the short- and long-range transport processes. When rainfall and substrate lithology are uniform, a significant amount of discharge draining over the escarpment top causes it to degrade. Only when the top of the model escarpment coincides with a drainage divide can escarpment retreat occur for these conditions. An additional requirement for retreat of a model escarpment without decline is a long reaction time scale for fluvial entrainment. This corresponds to a substrate that is hard to detach by fluvial erosion, and therefore to fluvial erosion that is not transport limited. Continuous backtilting of an escarpment due to flexural isostatic uplift in response to denudational unloading helps maintain the scarp top as a divide. It is essential if the escarpment gradient is to be preserved during retreat in a uniform lithology. Low flexural rigidities promote steep and slowly retreating escarpments. For given rainfall and substrate conditions, the morphology of a retreating model escarpment is determined by the ratio of the short-range diffusive and long-range advective transport efficiencies. A low ratio (which is interpreted to correspond to a relatively arid climate and weathering-limited conditions) promotes steep, sharp-topped escarpments with straight main slopes, and escarpment retreat occurs over a wide range of height scales. A high ratio (interpreted to correspond to a more humid, temperate climate) produces a convex upper slope, and concave lower slope morphology and only major escarpments are predicted to preserve a high scarp gradient. Lithological contrasts in the model produce more complex morphologies and predict the formation of scarps crowned by an erosionally resistant caprock. However, resistant caprocks are not an essential requirement for model scarps to retreat. We conclude that the inferred controls and model behavior are both consistent with the present-day morphology of rifted continental margins and with modern conceptual models of landscape evolution.

Introduction

Erosional escarpments are common features of rifted margins that have a high-elevation inland (Figure 1). The escarpments, which may be 1 km high and up to several hundred kilometers from the coastline, separate a low-elevation coastal area from the inland higher elevation area. Examples are the "great escarpments" of southwest Africa, southeastern Australia, eastern Brazil, and western India [*Ollier*, 1985].

Paper number 94JB00047.
0148-0227/94/94JB-00047$5.00

Ollier [1985] interpreted these escarpments to be genetically related to continental rifting. He suggested that they have retreated inland from the rift hinge zone since continental breakup when local baselevels dropped considerably and/or the margin flanks were uplifted. His ideas are similar to those of *King* [1953] and *Partridge and Maud* [1987], although they related escarpment initiation and retreat to multiple episodes of inferred surface uplift that are not specifically related to rifting [*Gilchrist et al.*, this issue]. These uplift episodes may have occurred, but the proposed causal mechanisms, delayed isostatic response to denudational unloading [*King*, 1955; *Partridge and Maud*, 1987] and/or cymatogeny [*King*, 1983], remain without a good physical basis.

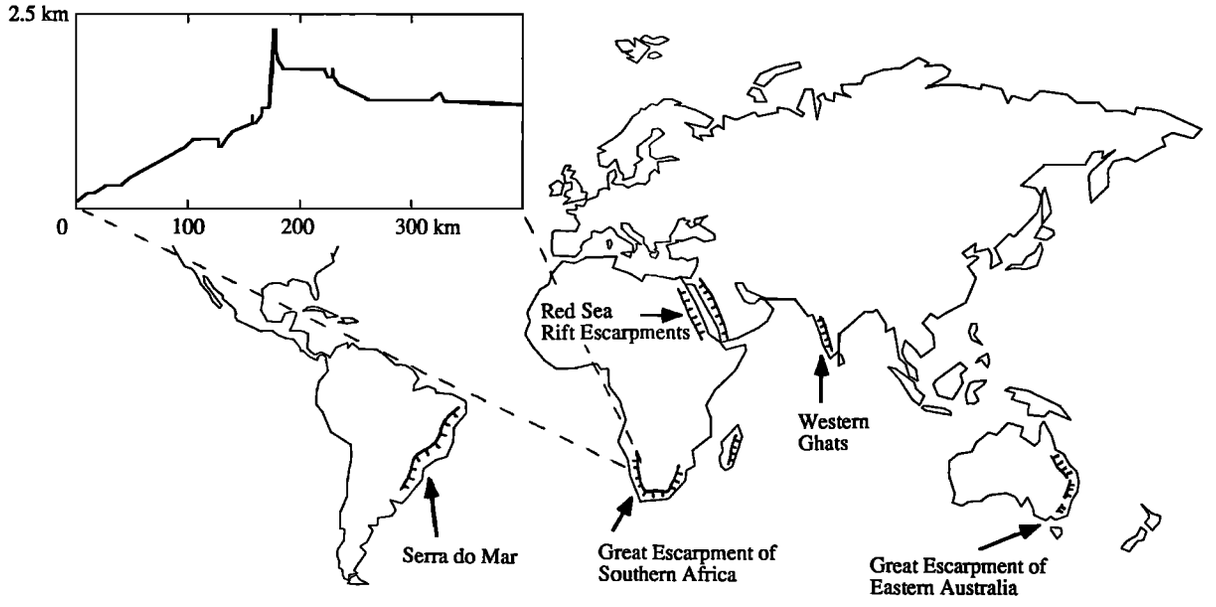

Figure 1. Map showing the locations of major erosional escarpments on rifted continental margins. The inset shows a typical topographic profile across the Great Escarpment of southwestern Africa.

Gilchrist and Summerfield [1990] list observations that support Olliers's interpretation. (1) Escarpments are semiparallel to the present-day coastline. (2) In the coastal areas, drainage is mainly toward the coast and perpendicular to the escarpment, while in the upland region, drainage tends to be more complex. This observation suggests that the escarpment captured the inherited drainage and created a seaward gradient as it retreated. (3) At the western margin of southern Africa the coastal area is characterized by high local relief, thereby promoting relatively high denudation rates, whereas inland of the Great Escarpment, local relief is very low, giving rise to low denudation rates despite the relatively high regional elevations [*Summerfield*, 1991]. (4) Apatite fission track data imply deeper denudation in coastal catchments than in the interiors [*Brown et al.*, 1990; *Bohannon et al.*, 1989; *Moore et al.*, 1986]. (5) Given the former greater westward extent of the Karoo Basin from southern Africa to Brasil, the exposure of older Karoo strata and basement rocks along the western margin of southern Africa indicates significant depths of erosion in this area. Conversely, the preservation of younger Karoo sediments and Cenozoic weathering profiles in the interior indicates much lower rates of post-rifting denudation inland of the escarpment.

Unfortunately, the observations do not resolve how the escarpments evolved on geological timescales, and the key question, whether Ollier's retreat interpretation is correct, remains unanswered. In this paper we take an alternative approach and investigate the factors that control escarpment evolution and retreat on rifted margins in a quantitative surface processes model. We then ask whether the model controls are also important in natural systems.

Modeling studies of large-scale long-term landscape evolution have not been undertaken until recently because the idea prevails that we must first understand the great variety of processes and complex behavior observed at small temporal and spatial scales in terms of physical laws and because it is computationally impossible to apply these laws and empirical transport relationships at large scales [e.g., *Dietrich et al.*, 1992].

As demonstrated in other sciences, a fruitful approach to such problems of scale is to set aside (for the time being) the small-scale, short-timescale picture and to explore simple relationships cast in terms of large-scale, long-timescale quantities. In thermodynamics, for example, the behavior of gases was first formulated in terms of properties associated with the collective behavior of molecules (pressure, temperature, and entropy) and not the interactions between individual molecules.

What are the appropriate thermodynamically equivalent transport laws for large-scale (order of 1-1000 km) long-term (order of 1-100 m.y.) landscape evolution? It is important to distinguish models developed for these large scales, such as the model employed in this study, from, for example, hydrological models of contemporary catchment flood hydrograph response and sediment yield [e.g., *Beven and Kirkby* , 1979; *Wood et al.*, 1990], although ultimately the two approaches must be reconciled.

A number of studies have explored the behavior of a single process, such as linear diffusion [e.g., *Culling*, 1960], or nonlinear transport that is a function of both area (or equivalently discharge) and gradient [e.g., *Sprunt*, 1972; *Smith and Bretherton*, 1972; *Armstrong*, 1976; *Cordova et al.*, 1983]. More recent studies include interactions among a small number of processes that are individually relatively simple [e.g., *Kirkby*, 1986, *Ahnert*, 1987, *Chase*, 1988;*Willgoose et al.*, 1991a,b]. The richness of the behavior of these models is derived from the interactions and not the basic processes alone. *Chase's* [1992] mobile cellular automaton is numerically simple and apparently captures some of the statistical properties of natural landforms. However, it is not clear how the model relates to continuous processes expressed in terms of differential equations. For example, fluvial entrainment has no spatial or time scale.

Willgoose et al. [1991a,b] developed a model based on continuum mechanics which includes overland and channelized

flows, a channel initiation function, and a fluvial transport formulation which depends nonlinearly on discharge and local slope. Discharge is calculated as a function of catchment area and the model uses transport-limited fluvial mass removal and deposition. That is, the rivers always carry at capacity. *Willgoose et al.* [1991a] demonstrated that hillslope evolution in their and other models that employ a transport-limited formulation [*Leopold and Langbein*, 1962; *Hirano*, 1968; *Ahnert*, 1976; *Begin*, 1987; *Shaw and Mooers*, 1988; *Chase*, 1988] can be broken down into a diffusive component, causing hillslope degradation, and a retreat component. These components are generally complex functions of local slope, discharge, and spatial divergence or convergence of discharge [*Smith and Bretherton*, 1972], and therefore hillslope evolution is similary complex.

Anderson and Humphrey [1990] used a model in which soil, produced by weathering, is transported by linear diffusion. The explicit formulation of weathering and the exclusion of bedrock transport in the model mean that denudation becomes locally controlled by the weathering rate when diffusive transport is faster than the production of transportable material. Since the weathering rates on a bedrock escarpment face are uniform in their model, an initial straight main slope is preserved and a component of parallel retreat results. They demonstrate that for weathering-limited transport on a 2-km-high model scarp, parallel retreat of the main slope (as defined by *Carson and Kirkby* [1972]) over several kilometers can occur, but due to ongoing main slope shortening, the scarp would degrade after some relatively short distance of retreat. This escarpment behavior is intermediate between the degradation of model escarpments without parallel retreat for substrates with uniform diffusive properties and the diffusive retreat of model escarpments armoured by a resistant, low diffusivity caprock.

This introduction leads to the following problems which this paper attempts to address. (1) What are the physical processes and properties that control escarpment preservation? (2) Do escarpments always have erosionally resistant caprocks? If not, what are the minimum requirements of process models that preserve and retreat escarpments without degradation when the substrate has uniform properties? (3) Of special interest is the question whether parallel retreat of escarpments is a mode of landscape evolution characteristic of models that are not a priori transport limited. If so, the behavior of bedrock rivers, in which fluvial entrainment is related to the detachability of the substrate, is critical to escarpment retreat.

In the following sections we describe the model, discuss the separate basic behavior of the hillslope and fluvial mass transport components, and then investigate, in one dimension, escarpment evolution arising from the interaction of these model components. Some of the model parameters that control the escarpment evolution are interpreted in terms of substrate properties and climate. Scarp development in two dimensions is then shown in contrasting model climatic conditions. Finally, the parameter values are discussed, and the relationships that have been obtained from the model experiments are evaluated in comparison with natural systems.

Surface Processes Model

The model is similar to the *Willgoose et al.* [1991a,b] model in that it employs both diffusive hillslope transport and fluvial transport in a drainage network that collects discharge. Our model differs from theirs in three ways. (1) It allows arbitrary rainfall distribution; therefore discharge is not solely proportional to area. (2) It does not distinguish between hillslope and channel elements. (3) It employs a fluvial transport formulation that includes a timescale or length scale for fluvial mass entrainment and deposition that depends on substrate lithologies. Mass removal is, therefore, not a priori transport-limited. These three properties are similar to *Chase's* [1992] model, but the primary difference is that the model discussed here is based on numerical solution of differential equations based on continuum mechanics and is not a "rules-based" cellular automaton.

The surface processes model describes the long-term changes in topography $h(x,y,t)$ as a result of simultaneous short- and long-range mass transport processes. It therefore addresses both the process and form components of the problem in an internally consistent manner. Calculations are made numerically by integrating the model differential equations on a uniform discrete topographic grid size of c_L. Process rates are assumed to be constant and at steady state during each model time step Δt. The landscape evolution is calculated by updating the topography at the end of each time step for the effects of denudation (and tectonic rejuvenation and isostatic readjustment, if these are included). A detailed description of the integration of the transport equations is given by *Beaumont et al.* [1992].

Short-Range Transport

The short-range transport represents the cumulative effects of hillslope processes (such as soil creep, rain splash, earth flows, slides, and rockfall) that remove material from hill and mountain sides and transport it to adjacent valleys [*Carson and Kirkby*, 1972]. On short timescales the magnitude-frequency distributions of mass movements of the various hillslope processes are distinctly different and some depend on threshold mechanisms. On long timescales addressed by the model they, however, share the characteristic that they distribute mass over a short distance and depend on local slope. Following *Culling* [1960, 1965], *Hanks et al.* [1984], *Pierce and Colman* [1986], *Andrews and Bucknam* [1987], and *Anderson and Humphrey* [1990], for example, we represent this short-range transport as linear downslope diffusion of material volume. The horizontal material flux q_s is related to the local slope ∇h by

$$q_s = -K_s \nabla h, \tag{1}$$

where K_s is the diffusivity. To be consistent with the simplifying assumptions used elsewhere in the model, we regard K_s as a material property and not as a continuous variable. We therefore assign different values of K_s to different lithologies, low values for intact bedrock that is not weathered and high values for cohesionless sediment.

The diffusivity K_s may be interpreted as $K_s = u_s h_s$ [*Beaumont et al.*, 1992], where h_s is the thickness and u_s is the transport speed of an erodible surface boundary layer. This interpretation becomes important later in the paper when the effect of climate on weathering rates and therefore on the thickness h_s of the weathered layer or regolith is considered. When the model climate implies rapid weathering, h_s and probably u_s of the bedrock increase. Therefore K_s may be interpreted as a function of both lithology and climate.

If it is assumed that there is no tectonic transport of the surface material, that volume is conserved (porosity changes

are ignored), and that the effects of solution are negligible, the transport equation can be combined with the continuity equation,

$$\frac{dh}{dt} = -\nabla \cdot q_s \tag{2}$$

to give the linear diffusion equation for the rate of change of local height, the denudation, in response to erosion by the short-range processes,

$$\frac{dh}{dt} = K_s \nabla^2 h. \tag{3}$$

Long-Range Transport

The long-range transport model represents the cumulative effect of fluvial transport. Fluvial transport is modeled by a network of one-dimensional rivers that drain the current model topography via their respective routes of steepest descent. Each river is no more than a corridor that transports mass among the cells of the discrete model topography. No attempt is made to distinguish river type or their dynamical characteristics. Instead, the local equilibrium sediment carrying capacity q_f^{eqb} of the long-range transport network is considered proportional to local linear river power [*Begin et al.*, 1981; *Armstrong*, 1980; *Chase*, 1992]

$$q_f^{eqb} = -K_f q_r \frac{dh}{dl} \tag{4}$$

where q_r is the river discharge per unit width, dh/dl is the slope in the direction of river drainage, and K_f is a nondimensional transport coefficient. q_r and q_f have dimensions (L^2/T) and therefore conform to the standard definition of fluxes. As explained by *Beaumont et al.* [1992, equation 19] the numerical calculations are made in terms of the integrated fluxes (L^3/T). The reader is therefore free to interpret the width to depth ratio of the model rivers in any way that is consistent with this approach. In the appendix we give the rationale for using linear capacity for the model rivers.

Fluvial discharge q_r is related to the net precipitation rate $v_R(x,y,t)$ by conservation of water over the upstream catchment area. That is, v_R represents the precipitation that contributes to surface runoff and recharges the river system. Evaporation and infiltration are ignored, although their effect could be added. In the models presented in this paper, v_R is uniform in space and time. No distinction is made between hillslope and channel elements because the large spatial scales and the low grid resolution do not allow such distinctions to be made in a realistic way.

The local sediment flux q_f transported by the rivers is determined by integrating a reversible entrainment-deposition equation down the river network. We adopt the view that the fluvial system must do work on the landscape in order to transfer material from the substrate into the transported sediment flux. This is represented in the model by a first-order kinetic reaction in which the reaction rate is proportional to a rate constant $1/t_f$ and to the degree of disequilibrium in the fluvial sediment flux as it moves in a Lagrangian sense (i.e., from the viewpoint of an observer moving with the advection velocity v_f of the sediment flux) along a river,

$$\frac{dq_f}{dt} = \frac{1}{t_f}\left(q_f^{eqb} - q_f\right) \tag{5}$$

From the point of view of an Eulerian observer who is fixed to the landscape

$$\frac{dq_f}{dt} = \frac{\partial q_f}{\partial t} + v_f \cdot \nabla q_f. \tag{6}$$

If the sediment transport is in steady state, that is, the fluxes do not vary with time during interval Δt, $\partial q_f / \partial t = 0$ and equation (6) reduces to $dq_f/dt = v_f \, dq_f/dl$. Under these circumstances the time dependence of erosion or deposition takes the form of a spatial dependence,

$$\frac{\partial h}{\partial t} = -\frac{dq_f}{dl} = -\frac{1}{l_f}\left(q_f^{eqb} - q_f\right) \tag{7}$$

where $l_f = v_f t_f$. For constant v_f, l_f is a material property, the erosion-deposition length scale required for the disequilibrium to be reduced to a factor of ($1/e$) when q_f^{eqb} is constant.

When $q_f < q_f^{eqb}$, the model river entrains material with an l_f that is inversely proportional to the detachability of the substrate. A low value of l_f corresponds to easily detachable material, such as unconsolidated material or model sediment previously transported by either the short- or long-range model components. When $l_f \to 0$ the reaction no longer limits sediment transport and (7) plays no role because $q_f \to q_f^{eqb}$ as predicted by the transport-limited capacity (4).

Bedrock is less readily detached or abraded and is associated with a low reaction rate. It is therefore represented by higher values of l_f than sediment. Where model streams in bedrock are strongly under capacity (i.e., $q_f << q_f^{eqb}$), equation (7) reduces to $\partial h/\partial t = -q_f^{eqb}/l_f = -(K_f q_r / l_f) dh/dl$. This is the linear equivalent of the relationship proposed by *Howard* [1980], used in empirical studies by *Howard and Kerby* [1983] and discussed by *Seidl and Dietrich* [1992]. It remains uncertain whether the reaction is accelerated by the sediment flux already transported by the river, as might be expected for abrasion. If true, this behavior would make the reaction autocatalytic on a short term. It can equally be argued that labile sediments, which armour channels, reduce the effect of abrasion on the bedrock. On a long-term statistical basis these sediments will be more prevalent where rivers approach capacity. For these timescales a form of the reaction in which the potential for detachment of the bedrock decreases as the carrying capacity is approached (i.e., equation (7)) is therefore appropriate.

When $q_f > q_f^{eqb}$, for example, where slopes decrease, sediment is deposited from the overcapacity model river and l_f, the deposition length scale, has a low value because there is no mechanical restriction on deposition. Sediment accumulation and the spatial variation of l_f values are recorded by the evolving model so that fluvial entrainment at a given location first removes the accumulated sediment with an appropriate l_f before attempting to detach bedrock with its corresponding l_f.

Although the present formulation does not describe the small-scale physics of bedrock erosion by abrasion or plucking, it provides a more general macroscopic description than an inherently transport-limited formulation which is limited in its applicability to easily detachable substrates and does not allow distinction between substrate lithologies for the fluvial system.

Basic Behavior of the Independent Model Components

Figure 2 illustrates the basic one-dimensional model behavior of the short-range and long-range mass transport components when considered independently. The initial topography consists of two uniform but unequal slopes dipping in opposite directions. Constant elevation boundary

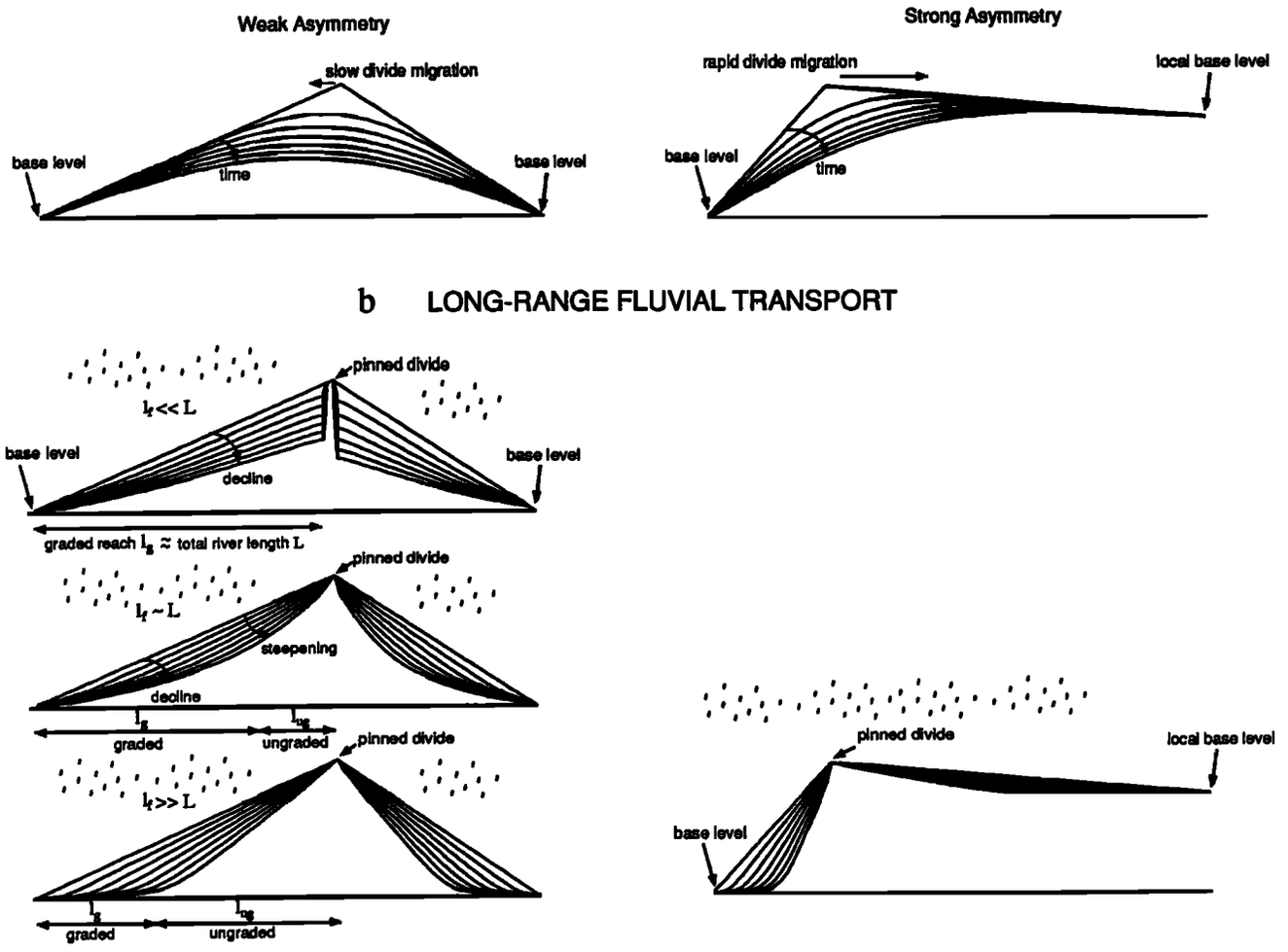

Figure 2. Basic model behavior of (a) short-range hillslope diffusive transport and (b) long-range fluvial transport. A detailed explanation is given in the text.

conditions are used which act as sediment sinks and simulate local baselevels of erosion. Denuded topography is not rejuvenated. Behavior is shown for both a weakly asymmetric and a strongly asymmetric topography. In the latter case the left- and right-hand local baselevels differ in elevation.

Short-Range Diffusion

Short-range hillslope diffusive transport (Figure 2a) leads to the following evolution: (1) smoothing of topography, (2) slope decline, (3) denudation of divides, and (4) lateral migration of drainage divides in the direction of the lower slope gradient. Topography is smoothed and slopes decline as a consequence of linear diffusion with a constant diffusivity because the denudation rate is proportional to the curvature of topography d^2h/dx^2 (where x denotes the horizontal spatial dimension in the one-dimensional models), which leads to preferential removal of high-frequency spectral components in the topography. Even though drainage divides may have zero slopes at their top, they are inherently associated with curvature of topography and are therefore denuded by diffusive mass transport. The diffusive sediment flux q_s tends to zero at a drainage divide, but it is the change of sediment flux dq_s/dx which determines the erosion, and this remains finite. A drainage divide migrates when the denudation rate at the divide changes from one side to the other. For a uniform diffusivity K_s this occurs when $d^2h/dxdt = K_s d^3h/dx^3 \neq 0$, that is, when the curvature of topography changes across the divide. The divide migrates toward the lower curvature side at a rate proportional to the change in curvature d^3h/dx^3.

In summary, diffusive migration of divides is controlled by the local curvature asymmetry. In the absence of other processes this asymmetry reflects the asymmetry of the adjacent hillslopes on a length scale $(K_s t)^{1/2}$, where t is the age of the divide. Divides do not migrate when the curvature is symmetric and they migrate more rapidly as the curvature asymmetry increases.

Long-Range Fluvial Transport

Long-range fluvial transport is shown for uniformly distributed precipitation. Both slopes in the one-dimensional model (Figure 2b) therefore contain rivers, without tributaries, in which fluvial discharge increases linearly from the divide to baselevel. The horizontal scale of the topography is characterized by the length L of the river draining to the left.

The long-range fluvial transport (Figure 2b) leads to the following evolution: (1) Drainage divides neither erode nor migrate (we refer to this as "pinned divides"). (2) A "graded river profile" length l_g is cut, grows headward, and causes slopes to decline. (3) Slopes of the ungraded reaches l_{ug} above l_g and around divides correspondingly steepen.

That drainage divides are pinned for long-range fluvial transport follows directly from equations (4) and (7). Both q_f^{eqb} and q_f tend to zero at divides because q_r tends to zero. Therefore dq_f/dl tends to zero as well, which implies no erosion. This behavior is consistent with the concept of a "belt of no erosion" by overland flow as used by *Horton* [1945]. Consequently, when there is no hillslope diffusion, long-range fluvial processes erode the model topography between drainage divides to baselevel but leave antecedent drainage divides unaffected. Ultimately, the topography takes the form of pinnacles and walls.

For strictly transport-limited fluvial erosion, where $l_f = 0$ and $q_s = K_f q_r dh/dl$, this pinning behavior does not occur. Under these circumstances the denudation rate is given by $dh/dt = K_f[\partial h \partial q_r/\partial l^2 + q_r \partial^2 h/\partial l^2]$. The first term describes parallel retreat at a rate $K_f \partial q_r/\partial l$. A divide is therefore eroded when at least one of its slopes is nonzero. *Carson and Kirkby* [1972] demonstrate in their Appendix C that for uniform rainfall the curvature at the divide tends to zero. Because q_r also tends to zero, the second term, which describes diffusion with diffusivity $K_f q_r$, does not contribute to divide erosion, and the behavior of the divide is completely determined by the first term. The slopes at the divide therefore neither steepen nor decline.

With regard to the concept of grade, *Mackin* [1948, p. 471] described a graded river as "a river in which, over a period of years, slope and channel characteristics are delicately adjusted to provide, with available discharge, just the velocity required for the transportation of the load supplied from the drainage basin". *Mackin* [1948, p. 471] further stated that "the graded stream is a system in equilibrium; its diagnostic characteristic is that any change in any of the controlling factors will cause a displacement of the equilibrium in a direction that will tend to absorb the effect of the change". These concepts are generally in accord with other definitions of a graded state [e.g., *Schumm*, 1977; *Morisawa*, 1985]. Both aspects of Mackin's description are intrinsic parts of the model behavior. The model fluvial system does cut a profile in which the slope is delicately adjusted for transportation of the sediment flux (load) supplied from the catchment upstream through to baselevel. In the graded region l_g of the model river the disequilibrium $(q_f^{eqb} - q_f)$ and, consequently, the erosion rate tend progressively to zero. However, equilibrium is not truly achieved in the model (Figure 2b), because the sediment flux from the ungraded catchment also changes with time. The entrainment/deposition reaction (equation (7)) plays the role of controlling the river's approach to a simultaneous equilibrium and graded state, $\partial q_f/\partial l \rightarrow 0$. This is the key to fluvial landform evolution in this model formulation.

The graded river profile in the model is first established at baselevel (Figure 2b) and grows headward at the expense of ungraded topography l_{ug} closer to the divide, a behavior that was already noted by *Gilbert* [1877] in natural systems. For $l_f << L$ (relatively high detachability and a short erosion length scale), grading and headward growth are efficient, the sediment yield is high, and the graded profile is cut with a high gradient to provide the carrying capacity necessary to transport the high sediment yield. In this limit, the graded profile corresponds to the characteristic form [*Kirkby*, 1971] to which slopes tend under transport-limited removal. For $l_f >> L$ (relatively low detachability and a long erosion length scale), grading and headward growth are inefficient, the sediment yield is low and the graded profile is cut with a low gradient to provide a relatively low carrying capacity for the small amount of sediment supplied from upstream. For $l_f \sim L$ the behavior is intermediate.

As graded reaches of the model rivers grow headward, the ungraded reaches l_{ug} steepen because divides are pinned under fluvial erosion. For $l_f << L$, steepening of divides is an efficient but local process. Steep slopes are established at divides after limited removal of the total erodible rock volume above baselevel (Figure 2b). For $l_f >> L$, steepening at divides is inefficient. Steep slopes are created at the divide only after most of the topography of the entire watershed has been removed, but these slopes span a large proportion of the watershed elevation because the graded reaches have low slopes.

Investigation of the Controls of Model Escarpment Evolution

An escarpment can be considered to be a limiting case of the initial topography used in the previous section. When the left slope (Figure 2) becomes steep and the right slope tilts gently down to the right or to the left, we have the basic one-dimensional initial configuration in which to investigate how the steep slope, the escarpment, evolves. We analyze the model escarpment behavior in one dimension as a function of the antecedent configuration, the erosion length scale of the bedrock substrate, the flexural isostatic response to denudation, and different combinations of the combined surface processes model. The rationale for the range of values of the surface processes parameters that is investigated is discussed in the discussion section. The purpose of these illustrative models is to determine the circumstances under which model escarpments are preserved or retreat across the model without declining.

Role of Antecedent Drainage and Erosion Length Scale

Figures 3 and 4 display model results for the two basic styles of antecedent topography, that is, where the drainage divide is located inland of the escarpment and where the drainage divide coincides with the escarpment top, respectively. The starting set of surface processes parameter values for the sensitivity analysis is given in Table 1. In the

Table 1. Starting Model Parameter Values

Parameter	Value
K_s (bedrock)	0.5 m²/yr
K_s (sediment)	5.0 m²/yr
$K_f v_R$	0.01 m/yr
l_f (sediment)	100 m for $c_L < l_f$
	c_L for $c_L \geq l_f$

models of Figures 3 and 4, only the erosion length scale of the basement rock varies. The precipitation is uniform in time and space, and therefore we have chosen to characterize the model by the product $K_f v_R$ which gives a measure of the fluvial transport efficiency. Both boundaries have constant heights. The left boundary is interpreted as sea level or the baselevel of denudation, whereas the right boundary is the baselevel for a stable inland watershed. Sediment flux leaves the model through these boundaries. Escarpment evolution can be understood by combining the separate behavior for hillslope and fluvial transport described in the previous section.

Drainage divide inland of escarpment, no isostatic response to denudation. In the models of Figure 3 a divide is effectively positioned at the right boundary and the upland between the divide and the escarpment is drained over the escarpment. The evolution of the model scarp is best understood in terms of the two components in the discharge on the escarpment; the discharge from precipitation on the scarp face q_r^{os} and the discharge collected above the scarp q_r^{as}. The effect of q_r^{os} is identical to its contribution to the behavior of slopes at drainage divides (see Figure 2b). It acts to steepen the escarpment as a downstream graded region is created. The second component q_r^{as} causes erosion of the scarp top and leads to a combination of retreat and decline of the escarpment face. For low l_f (Figure 3a), erosion due to q_r^{as} is local and in proportion to the change in slope. This corresponds closely to diffusive behavior. The retreat component is therefore subdued relative to diffusive smoothing and slope decline. As l_f increases (Figures 3b and c), erosion due to q_r^{as} is progressively more evenly distributed in a downstream direction over the scarp face and beyond, leading to a more effective retreat component. The role of diffusion in these models is relatively unimportant except if K_s is chosen very large, in which case it enhances smoothing and slope decline.

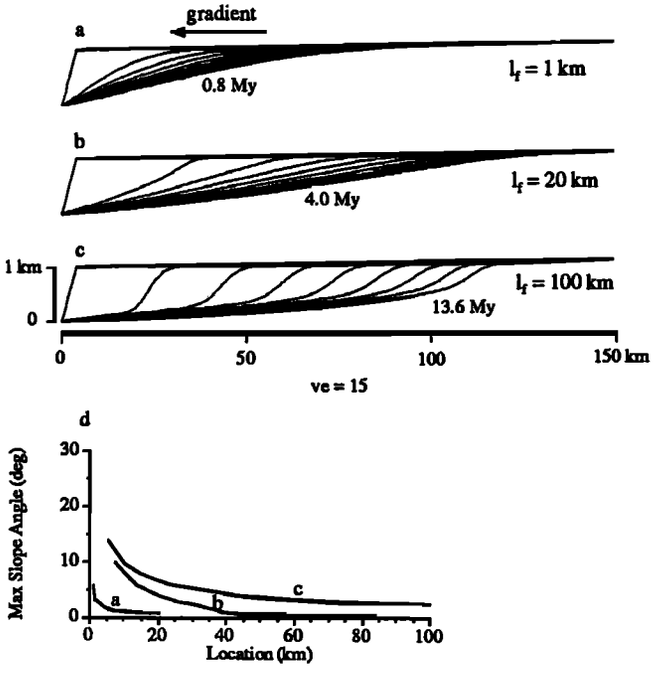

Figure 3. Model escarpment evolution of the type where the drainage divide is located inland of the escarpment and flexural isostasy is not included. The escarpment is 1 km high and slopes at 45°. Topographic profiles for three erosion length scales, l_f, at equal time increments of (a) 0.1, (b) 0.5, and (c) 1.7 m.y., respectively. (d) Maximum slope angle of the escarpments in Figures 3a-3c as they evolve through time against the distance from the left baselevel. Grid size c_L=500 m.

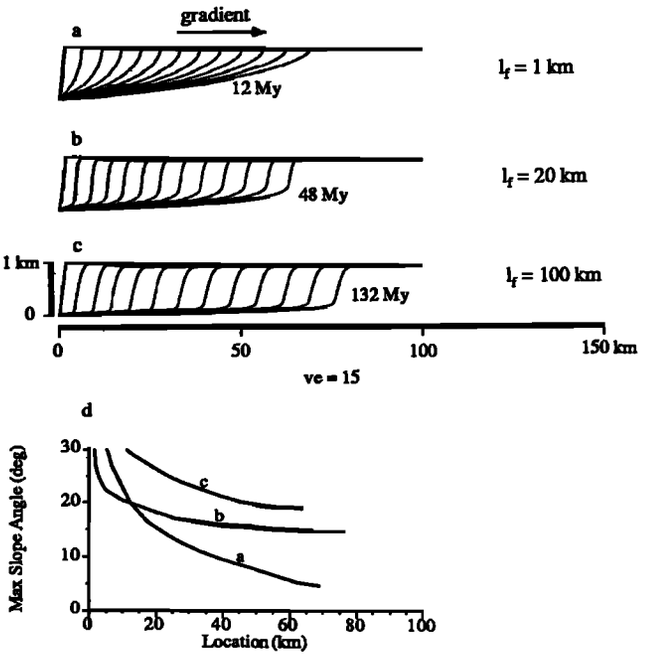

Figure 4. Same as Figure 3 for escarpments of the type where the drainage divide coincides with the top of the escarpment. Topographic profiles for time increments of (a) 1, (b) 4, and (c) 11 m.y., respectively. Grid size c_L=50 m. (d) Maximum slope angle of the escarpments in Figures 4a-4c as they evolve through time against the distance from the left baselevel.

Escarpment evolution for models with an inland drainage divide therefore reflects a competition between q_r^{os}-powered steepening and q_r^{as}-powered retreat and slope decline. The potential for escarpment preservation for these models is not good as shown by the maximum slope angles in Figure 3d. This is particularly true for low l_f (Figure 3a) where steepening by q_r^{os} only occurs at the scarp top and q_r^{as}-powered "diffusion" is strong. The preservation potential improves for increasing l_f (Figures 3b and c) which also promotes a low gradient graded section below the escarpment. Besides l_f, the distance from the escarpment to the drainage divide also plays a role in the escarpment evolution because it controls the relative importance of q_r^{as} and q_r^{os}. For the distal divides of the models shown, q_r^{as}, and its effect, retreat, and decline, dominate steepening by q_r^{os}. However, as the escarpments approach a drainage divide and the relative importance of q_r^{as} and q_r^{os} is reversed, they start to steepen.

It may be of interest to note that the models of Figure 3 resemble knickpoint evolution in a one-thread river [e.g., *Gardner*, 1983] where low l_f leads to rapid decline of the knickpoint face and smoothing of the overall knickpoint form without significant upstream migration, but increasing l_f, which corresponds to decreasing bedrock detachability, leads to better knickpoint preservation and upstream migration.

Drainage divide coincides with escarpment top, no isostatic response to denudation. In the models

of Figure 4 the top of the escarpment is the drainage divide, and the upland surface drains to the right. The evolution of the models can be understood by first considering the interaction of hillslope and fluvial processes at the top of the escarpment and then the role of l_f.

Hillslope diffusion migrates the escarpment top inland, in response to the asymmetry of the topography, and causes slope decline (see Figure 2a). At the same time the fluvial transport steepens the escarpment face as it cuts a downstream graded region (Figure 2b), but it does not erode the top of the escarpment. Consequently, in the vicinity of the top of the escarpment there is a competition between the rate of slope decline by diffusion r^{dec} and the rate at which slopes steepen by fluvial transport r^{st}. These rates depend on several factors. r^{dec} depends on the local character of the topography and the hillslope diffusivity, while r^{st} depends on the distance from the divide, the erosion length scale, and the topographic and precipitation characteristics of the watershed.

The models (Figure 4) show that the competition leads to an escarpment form that tends to a dynamic equilibrium in which each point on the escarpment has $r^{dec} = r^{st}$. A constant form at the top of the escarpment implies a constant rate of migration of the divide because the local asymmetry is maintained. Thus the surface processes not only stabilize the escarpment form but also its retreat rate.

Model results also show that escarpment form depends on the evolutionary relationship between its face and the graded region at its base, factors controlled by l_f. Small l_f gives the same behavior shown in Figure 2b in which a relatively steep graded region is created, and therefore the height of the escarpment decreases as it retreats (Figure 4a). In the limit l_f=0, that is, when the rivers transport at capacity, no distinction between escarpment and the downstream graded region can be made, and the initial escarpment evolves as a declining concave graded profile because $r^{st} \leq 0$; that is, the component of fluvial steepening is absent. In contrast, when l_f is large (Figure 4c), the escarpment retreats more slowly, the sediment flux is smaller, and the graded region has a lower slope, like that of Figure 2b with large l_f. The retreat is slow because the large l_f makes r^{st} small at the top of the escarpment; and, consequently, r^{dec} and the asymmetry are small, and the rate of diffusive divide migration is low. The key to a model escarpment that retreats over an appreciable distance without significant degradation is the dual role of a large l_f in limiting scarp steepening rate near the top and creating a low-angle graded region.

Although the form of the escarpment in Figure 4c remains relatively steep, Figure 4d shows that its maximum slope decreases slowly as it retreats. Figure 4c shows that the escarpment height also decreases because the slope of the graded region, although small, is finite. Slope decline occurs because a truly constant form cannot be maintained at the top of the escarpment. The upland above the escarpment becomes progressively flatter under fluvial denudation of the dip slope. This tendency increases the asymmetry at the top of the escarpment and increases the rate at which the divide migrates. The whole system responds by gradually changing the escarpment form, and this change includes a reduction of the maximum slope angle. Conversely, were fluvial denudation to incise the upland dip slope and increase its slope, the asymmetry would decrease and the rate of escarpment retreat would decrease. This evolutionary style is illustrated for a planform example by *Gilchrist et al.* [this issue].

Table 2. Parameter Values for Flexural Isostasy Calculations

Parameter	Value	Definition
E	7×10^{10} N/m	Young's modulus
ν	0.25	Poisson's ratio
ρ_c	2500 kg/m^3	Density (surface) crustal rock
ρ_m	3200 kg/m^3	Density mantle rock
g	9.8 m/s^2	Gravitational acceleration

Role of Flexural Isostasy

The previous two sets of models illustrated model escarpment evolution for two basic styles of antecedent topography and drainage. In the next two sets of models (Figures 5 and 6), flexural isostatic uplift in response to unloading is added to these basic styles. A uniform effective elastic thickness T_e is used. Other pertinent parameter values for the flexural calculations are given in Table 2. Although the total length of the models is 400 km, to maintain legibility only 150 km is shown in the figures. The right model boundary moves vertically with the isostatic motions and like the previous models is unerodible. The left boundary has a constant elevation. Both boundaries transmit the sediment fluxes. The starting set of parameter values (Table 1) is used for the surface processes.

Flexural loading by sediment deposited outside of the modeled region is not included. We justify this omission by noting that loads at a distance of one flexural parameter from the escarpment have an effect at the escarpment that is -1/e of equivalent denudation at the escarpment. This implies that sediment deposition can modify the early evolution of the models we discuss but that the changes will generally be minor once escarpment retreat equal to the flexural parameter has occurred. The purpose of the models is to illustrate the general denudational response. In regional model studies, where the history of sediment deposition and other potential loading processes are known, their effects are easily incorporated into the models [*Johnson and Beaumont*, 1994].

Antecedent flat upland plateau above the escarpment. These models (Figure 5) start with a flat plateau area above the escarpment so that the position of the initial drainage divide neither coincides with the top of the escarpment nor has a distal inland location. The addition of flexural isostasy has two important effects on the evolution of the models. First, it significantly enhances the depth of denudation because "graded profiles" must be cut into the isostatically uplifting crust. This effect has important implications for the large-scale magnitude of denudation and its chronology [*Gilchrist et al.*, this issue]. Second, the flexural isostatic uplift gradually increases the elevation of the escarpment and backtilts the upland inland of the escarpment. The backtilting imposes a definite drainage regime, with the escarpment top as drainage divide, on what was otherwise a flat, poorly drained upland. This is important for the morphology of the evolving escarpment.

Once the drainage divide has been established by the backtilting, the model topography in the vicinity of the

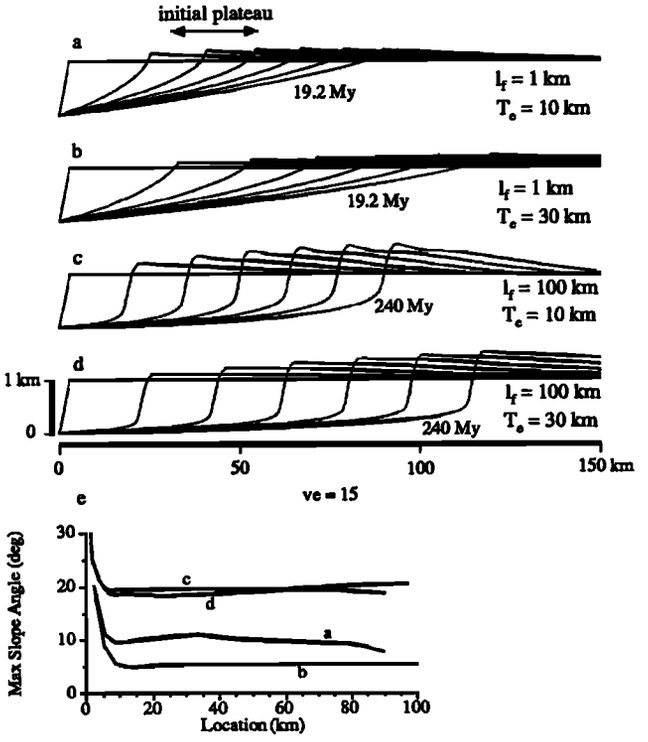

Figure 5. Model escarpment evolution of the type where the antecedent upland is a plateau and flexural isostasy is incorporated. (a)-(d) Topographic profiles for combinations of values of the erosion length scale l_f and effective elastic thickness T_e at equal time increments of 3.2 (Figures 5a and 5b) and 40.0 m.y. (Figures 5c and 5d). (e) Maximum slope angle of the escarpments in Figures 5a-5d as they evolve through time against the distance from the left baselevel. Grid size c_L=125 m.

escarpment evolves to a constant form (Figure 5) in which the rate of tectonic uplift and tilting is balanced by the rate of denudation. Values of T_e were chosen that are relatively low in order to illustrate this effect clearly. The isostatic backtilting is important because, together with the other processes, it acts to preserve a constant asymmetry at the top of the escarpment, a condition that prevents the gradual slope decline seen in models that ignore isostasy (Figure 4d). Low flexural rigidities cause strong backtilting, lower the asymmetry of the escarpment top and, consequently, promote low rates of escarpment retreat (Figure 5b and 5d). Tectonic uplift of the escarpment also assists in preserving the escarpment height as it retreats (Figure 5c and 5d). The concept of grade does not apply very well to the downstream regions in these examples because this region must be constantly denuded wherever it is isostatically uplifting and therefore cannot satisfy the definition of grade.

Antecedent upland drainage toward the escarpment. In the previous models (Figure 5) it was shown that isostatic uplift imposes a drainage divide that coincides with the escarpment top on an upland that was initially a poorly drained plateau. The models of this section (Figure 6) demonstrate that under some circumstances the same isostatic response can reverse upland drainage that was initially over the escarpment. The models (Figure 6) have the same initial geometry as those of Figure 3. Figure 3c shows the large l_f model evolution without isostasy, and Figure 6 illustrates the equivalent behavior for large to moderate values of T_e.

For high flexural rigidities, T_e = 90 km (Figure 3a), uplift and backtilting are insufficient to reverse the upland drainage, but for T_e of 60 km and 30 km (Figure 6b and 6c), drainage of the upland is reversed after some distance of retreat. The drainage reversal is accompanied by a transition of the escarpment behavior to the mode in which the escarpment top coincides with a drainage divide; and, consequently, the retreat rate decreases, and the escarpment steepens (Figure 6d).

The drainage reversal and accompanying change in escarpment behavior in the models are a consequence of the dynamical interaction between the denudation during escarpment evolution and its isostatic consequences. The change in mode of evolution depends not only on T_e but also on the initial gradient of the upland, the value of l_f, the need for a quasi-parallel retreat when the complete planform is considered, and sediment loading outside of the model area. Drainage reversal is favored by a planar upland with a low initial slope toward the escarpment, a large l_f and a small K_s.

Influence of Diffusive and Fluvial Processes on Escarpment Form

We now examine escarpment morphology and retreat rate in relation to K_s and $K_f v_R$. Other conditions are from the model of Figure 5d (initial upland plateau, l_f = 100 km, and T_e = 30 km).

Figure 7 shows that when l_f, T_e, and the height of the initial escarpment, H, are constant, the morphology of the retreating

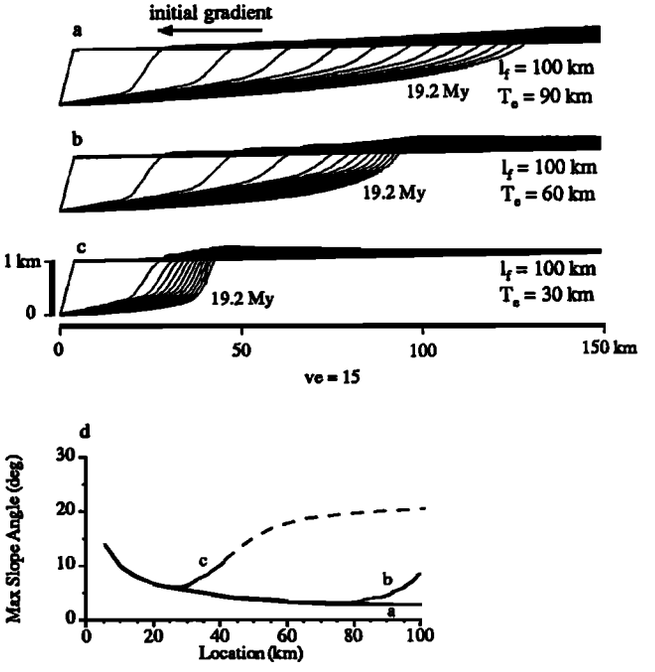

Figure 6. Model escarpment evolution of the type where the drainage divide is located inland of the escarpment and flexural isostasy is incorporated. (a)-(c) Topographic profiles for l_f=100 km and three values of T_e at equal time increments of 1.6 m.y. (d) Maximum slope angle of the escarpments in Figures 6a-6c as they evolve through time against the distance from the left baselevel. The dashed segment is the expected behavior for Figure 6c which was not calculated, but estimated using Figure 5d. Grid size c_L=500 m.

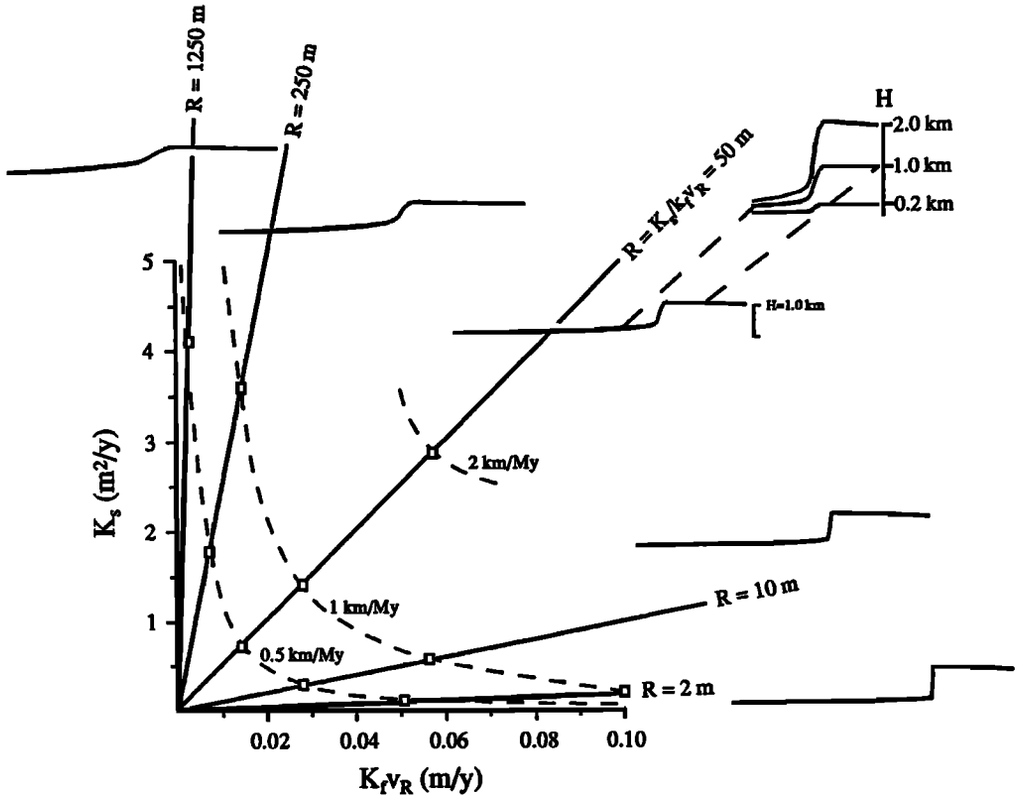

Figure 7. Escarpment morphology and retreat rate as a function of K_s and $K_f v_R$ and the combined parameter $R=K_s/K_f v_R$. Heavy solid lines are lines of constant R and constant morphology. R=50 m corresponds to the starting set of parameter values (Table 1). Dashed lines are contours of equal retreat rate. The top right part of the figure illustrates the effect of the height of the initial escarpment, H, on escarpment morphology for R=50 m.

escarpment is determined by $R = K_s/K_f v_R$, the ratio of diffusive to fluvial efficiency. R is a measure of the distance d_f from the escarpment top where diffusive and fluvial fluxes are equal ($q_f = q_s$). Diffusive and fluvial transports dominate for distances smaller than and greater than d_f, respectively. d_f is a function of the erosion length scale, precipitation distribution, and convergence and divergence of flow in planform models. For the above models, d_f=R in the limit that l_f tends to zero and as l_f increases, d_f becomes progressively greater than R.

For large R and $d_f > H$ (Figure 7), the scarp is diffusion dominated and is therefore convex upward in shape over much of its height. This leads to a low gradient, smooth convexo-concave scarp morphology and a relatively high gradient downstream graded region (see, for example, R=1250 m). Conversely, for small R and $d_f < H$, the scarp is only diffusion dominated near its top. The scarp has a high gradient and linear slope with a sharp top, distinct scarp base and a relatively low gradient downstream graded region (see, for example, R=2 m).

The escarpment gradient also depends on H (Figure 7, R=50 m). The higher the escarpment, the steeper it becomes. The relative roles of H and R imply that when R is large steep gradients only occur when H is very large, that is for major escarpments. In contrast, for small R, steep scarp gradients are predicted for wider range of heights.

Contours of equal escarpment retreat rate (Figure 7, dashed lines), where the rate is measured for the slope inflection point of the scarp, show that when R is constant, the retreat rate scales linearly with K_s and $K_f v_R$. This result follows from equations (3) and (5) because the denudation rates are a linear function of K_s and $K_f v_R$, respectively.

Influence of Lithological Contrasts

Lithological contrasts, particularly the effect of erosionally resistant caprocks, are often cited as the cause of natural escarpments. It is therefore important to investigate their behavior in the models where K_s and l_f depend on lithology. The model of Figure 5d (upland plateau and T_e=30 km) was used as a basis.

The first model (Figure 8a) has three horizontal layers in which l_f increases and K_s decreases with depth by factors of 5 between layers. The behavior of the model combines the rapid retreat and decline characteristic of the easily eroded top layer with constraints caused by local baselevels which are controlled by the underlying layers. These baselevels are lithologically controlled knickpoints and their behavior resembles that of escarpments where the upland drains toward the escarpment (Figures 3 and 6). In this model (Figure 8a), however, the drainage divide is not located at a fixed distal location. Instead, it migrates upstream by the headward retreat of the escarpment in the surface layer.

Initially, the escarpment top and the knickpoints retreat at different rates with the retreat rate increasing with increasing erodibility. After this initial phase a form of dynamical coupling develops between the divide and the knickpoints and

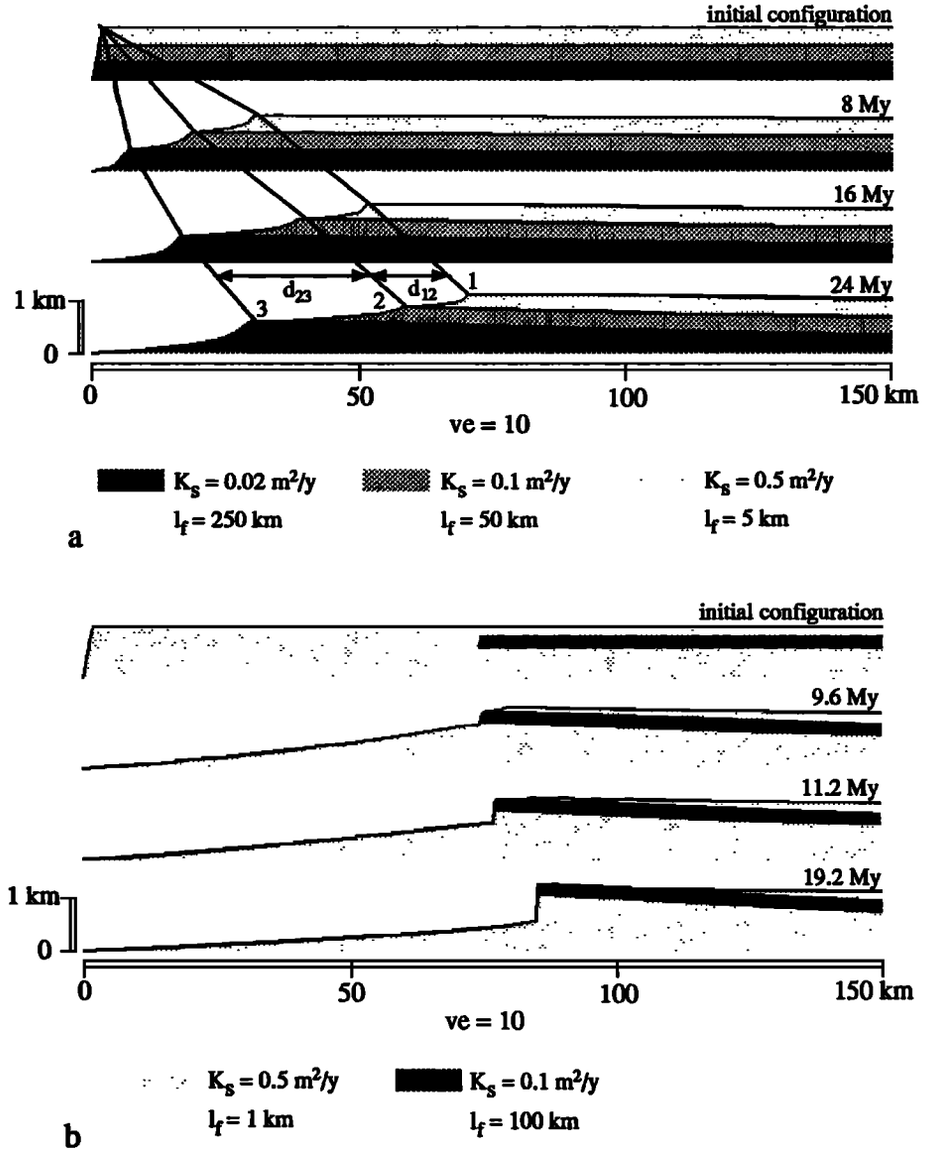

Figure 8. Two basic styles of effects of a horizontally layered substrate with lithological contrasts. (a) Decreasing erodibility with depth. The solid lines indicate that after an initial phase, a form of dynamical coupling develops between the divide (1) and the lithologically controlled knickpoints (2) and (3), in which they retreat upstream at approximately the same rate and constant forms develop for the segments d_{12} and d_{23}. (b) Exhumation of a truncated erosionally resistant layer that is buried beneath the upland plateau and takes the role of an resistant caprock.

all knickpoints retreat upstream at approximately the same rate. This behavior can be understood by considering the relationships between the layers taken in pairs. Point 1, the divide (Figure 8a), retreats according to the "escarpment top is a divide" controls discussed earlier. The retreat rate of point 2 is a function of $q_r(2)$, the discharge collected along d_{12}. Point 2 therefore lags behind point 1 until d_{12}, and therefore $q_r(2)$, become sufficiently large that point 2 achieves the same retreat rate as point 1. Thereafter, d_{12} remains the same and the 1-2 segment retreats through the upland as a constant form (Figure 8a). This form is similar to the early stages of Figures 5a and 5b, but it no longer depends on time. Instead, the distance d_{12}~10 km determines the form. The separation d_{23} at which point 3 also retreats at the same velocity as points 1 and 2 is explained in the same way because the velocity of point 3 is a function of $q_r(3)$. The underlying model behavior is important because it implies that forms are apparently arrested at a juvenile stage of their development and that there is a dynamical coupling among them. This raises the question whether similar steady state forms exist and retreat in natural systems.

The second model (Figure 8b) examines the effect of the denudational exhumation of a truncated, erosionally resistant layer, like a sill, that is buried beneath the upland plateau. The initial conditions and early evolution are like those of the models shown in Figures 5a and 5b. Once the resistant layer is exposed, the model passes through a phase in which the divide and the top of the resistant layer are linked as points 1 and 2 in Figure 8a. At the same time, the exhumed layer acts as a resistant caprock that controls the growth of a steep

escarpment in the underlying easily detached substrate. The flexural inland tilting in response to the unloading causes the drainage divide to migrate to the edge of the resistant layer. The final behavior is like that of the fluvial system acting alone on a small l_f substrate (Figure 2). The low K_s of the caprock is the key parameter because it limits the retreat rate of the divide and prevents an evolution like that shown in Figures 5a and 5b.

In summary, although these two models are only a superficial examination of the lithological effects, the implications are that lithology can play a major role in the formation of model escarpments. The earlier results, however, demonstrate that model escarpments also develop in uniform substrates. Resistant caprocks are therefore best regarded as accentuating the model styles found in uniform property substrates.

Reinterpretation of Model Escarpment Behavior in Terms of the Combined Control of Substrate and Climate

The one dimensional models of the earlier sections show that for a given antecedent topography which includes an escarpment, uniformly distributed rainfall, and the isostatic response of the lithosphere, it is the surface processes model parameters l_f and R that control model escarpment evolution. In this section we give an interpretation of these control parameters in terms of substrate and climatic conditions. This interpretation is illustrated in Figure 9.

We begin by extending our interpretation of l_f, the detachability of the substrate for fluvial entrainment. A very low l_f corresponds to a very high detachability (cohesionless fine-grained soil) (Figure 9). This end-member corresponds to a situation in which the fluvial system does not have to do much work on the landscape to entrain material from the substrate and may be equated with the more widely used term, "transport limited," because it implies that the fluvial system always carries at capacity (equation (4)) everywhere in the model landscape. The other end-member, a very high l_f, corresponds to a situation in which the fluvial system has to do a lot of work by processes such as abrasion and plucking to entrain material from the substrate which has a very low detachability. A high l_f therefore indicates fluvial-bedrock interaction. We do not interpret a high l_f to indicate that no sediment or regolith develops in the model landscape. As explained earlier, the fluvial transport component of the model first removes sediment created by the model from a given location before entraining the low detachability bedrock. This means that at a large scale the model can operate in a "weathering limited" regime, in which hillslope processes provide insufficient sediment to the valleys to prevent fluvial entrainment of the bedrock, or in a "transport-limited" regime in which the sediment supply to the valleys satiates the rivers which transport at capacity in a way that is not inhibited by the reaction length scale.

$R=K_s/K_f v_R$ provides a measure of the relative efficiency of hillslope diffusive processes and fluvial transport in the model. In the limit l_f tends to zero, d_f, the distance from divides for which slope diffusive processes dominate, tends to R. The $K_f v_R$ term in R is directly related to model climate in that it is proportional to precipitation. What is not so obvious is that $K_s = u_s h_s$ (see equation (1)) contains a climatic component. Weathering is responsible for the creation of a regolith in which cohesion has been destroyed, and it is this regolith, thickness h_s, that is involved in hillslope diffusive processes. Similarly, groundwater and soil saturation, climatically dependent variables, will influence u_s. Although we do not explicitly include weathering in the model, we make the interpretation that high values of K_s either represent lithologies that intrinsically diffuse easily, because they have low or no cohesion, or that weathering produces a cohesionless regolith sufficiently rapidly to satisfy the continuous denudation of the hillslopes with a high effective K_s. A thick, moist regolith will tend to produce high diffusivities, whereas a poorly developed dry regolith and bedrock will have low diffusivities. We use "tend" because other factors, for example, vegetation, will limit diffusion of an otherwise thick moist regolith.

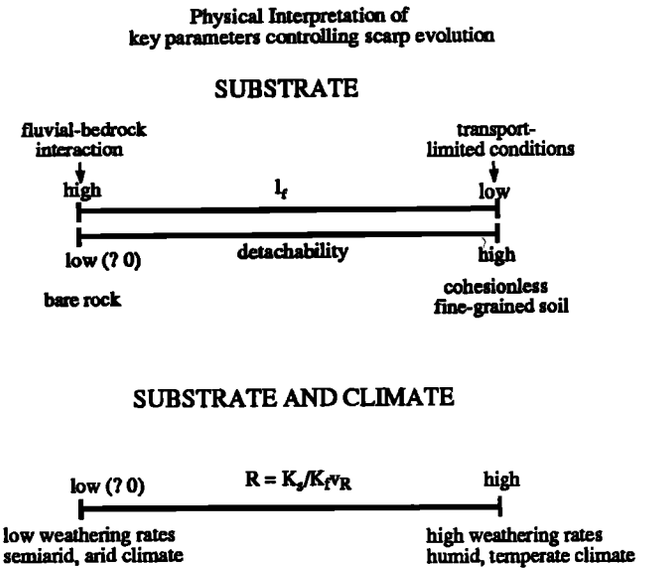

Figure 9. Interpretation of l_f and R in terms of model climate and substrate conditions.

Humid temperate climates with high precipitation rates are expected to have high K_s and $K_f v_R$ values and therefore will produce rapidly evolving model morphologies, except when limited by vegetation. Conversely, arid landscapes have low values of K_s and $K_f v_R$ and evolve slowly.

We interpret the effect of climate to be greater on diffusive process than on fluvial capacity. This interpretation implies that increasing aridity will decrease weathering, for example, more than it decreases fluvial transport. Consequently, R is smaller, and the model develops a rougher, more angular landscape. Extremely arid model landscapes will cease to evolve and climate changes will produce transient morphologies that may persist for geologically significant time scales.

Influence of Lithology and Climate in Planform Models of Escarpment Retreat

The one-dimensional models are deficient in the sense that they do not address the effects of divergence and convergence of flow which is an important aspect of natural landscape evolution. In this section we present two planform (two-dimensional) models to illustrate the evolution of model escarpments under contrasting model climatic conditions.

The initial topography (Plates 1 and 2) is the two-dimensional equivalent of the one used in the models of Figure 5. A uniform 1-km elevation continental margin is bordered on one side by an escarpment which drops to sea level over a distance of 2 km. The model is 50 km wide parallel to the coast and extends 150 km in the inland direction. The grid-size c_L=1 km. A white noise topography, amplitude of 25 m, is superimposed to create an initial two-dimensional drainage network. This noise creates a random, largely internal, drainage on the plateau. The imposed network subsequently organizes itself in response to the denudational processes and isostasy.

Reflective boundary conditions for model fluxes are used on the sides perpendicular to the scarp. The base of the initial scarp is kept at a constant sea level elevation and acts as the baselevel for erosion through which sediment is removed from the model. The opposite, inland boundary is unerodible but allows the passage of the sediment flux. Its elevation changes with isostatic vertical motions. This boundary therefore acts as an elevated local baselevel in the continental interior. The isostatic response is calculated by averaging denudational unloading and sedimentary loading for each model time step in the strike direction, applying this load to a one-dimensional elastic flexural beam overlying an inviscid fluid, and then correcting the topography by the predicted beam displacement. The isostatic displacement is applied uniformly in strike direction which is a good approximation for these models where the deviations from a one-dimensional configuration occur at wavelengths much smaller than the flexural wavelength. A T_e of 30 km is used in the models. The precipitation rate is uniform in both space and time.

The first result (Plate 1) represents the model response to relatively arid climatic conditions (starting values given in Table 1 and l_f=100 km for bedrock). These parameter values represent the most arid climate that can be computed in approximately two days with a 1-km grid size on an HP Apollo 720 workstation. More arid conditions, which correspond to lower values of R, require increased spatial resolution because the characteristic slopes are steeper, and increased spatial resolution, in turn, requires increased temporal resolution. Plate 1 shows that the starting parameter values predict the retreat of a relatively steep escarpment that is similar to the equivalent one-dimensional model (Figure 5d).

The second result (Plate 2) represents the model response to more humid, temperate climatic conditions produced by increasing the values of $K_f v_R$ and K_s by factors of 1.5 and 20 respectively, relative to the starting values, while l_f remains unchanged. This change increases R by approximately one order of magnitude. The initial escarpment declines to a relatively low angle feature (note the significant vertical exaggeration in the plates) and the topography is characterized by more rounded low angle convexo-concave hillslopes (Plate 2) than the previous model (Plate 1) because the distance from divides over which diffusion dominates has increased.

Plates 1 and 2 show two new aspects of model escarpment evolution. First, the two-dimensional morphology of the escarpment shows embayments and salients along the escarpment face. These features are the result of the antecedent topographic noise and the local topography in the area above the escarpment produced by erosion during escarpment retreat, which together cause the rate of diffusive divide migration to vary along the escarpment top. River valleys in the area above the escarpment are progressively beheaded. The salients are ridges, or interfluves, on which divergence of flow occurs, and they are diffusion dominated. Convergence of flow occurs in the embayments, but despite the advantage of a greater fluvial discharge, they do not grow unstably, probably because fluvial carrying capacity in the model only increases linearly with drainage area for a given gradient [*Smith and Bretherton*, 1972; *Kirkby*, 1986]. The salients and embayments develop a characteristic form, but they do not remain stationary on a particular section of the scarp. Instead, their location fluctuates in a dynamic way along the scarp face as conditions at the top of the escarpment change. The escarpment in these models remains relatively straight at the largest scale because there is no opportunity for the fluvial system to capture a large drainage area above the escarpment. The same limitation also causes the predominant drainage direction of the coastal catchment to be approximately orthogonal to the escarpment, which produces the relatively smooth downstream graded planated region. In these examples the regions below the escarpment can be termed pediments and pediplains because they are created in the manner envisaged for these morphological elements.

The second difference with respect to the one-dimensional models is a somewhat higher escarpment retreat rate for the same model parameters. The rate of escarpment retreat in the model of Plate 1, for example, is higher than the retreat rate in the model of Figure 5d. This is not surprising because the increased local relief afforded by the greater dimensionality of the planform model leads to higher denudation rates.

The two planform models presented in this section and the additional planform models of *Gilchrist et al.* [this issue] confirm that the controls on model escarpment evolution remain the same as those for one-dimensional models, provided that the initial geometry is close to a one-dimensional form. The divergence and convergence of flow and their feedbacks on different parts of the model escarpment do, however, lead to more complex scarp morphologies, a more dynamic escarpment evolution, and a somewhat higher retreat rate than in one-dimensional models.

Summary of the Controls of Model Escarpment Evolution

This section gives a summary of the controls of escarpment evolution for the surface processes model. Apart from the last point these controls apply to uniform rainfall and substrate conditions.

1. Antecedent topography, in particular the location of drainage divides relative to the escarpment, exerts a first-order control on escarpment evolution.

2. When the escarpment and drainage divides are widely spaced, so that a significant amount of discharge drains over the escarpment top, the escarpment declines to a low-angle feature without much retreat.

3. For escarpment retreat to occur, the top of the escarpment must be a drainage divide, although this is not a sufficient condition.

4. The key to preservation of escarpment slopes and, therefore parallel retreat, is the competition between diffusive slope decline and fluvial slope steepening that occurs in the vicinity of the escarpment top when it is a drainage divide.

5. During erosion of an escarpment that has a divide at its top, continuous backtilting of the escarpment due to flexural

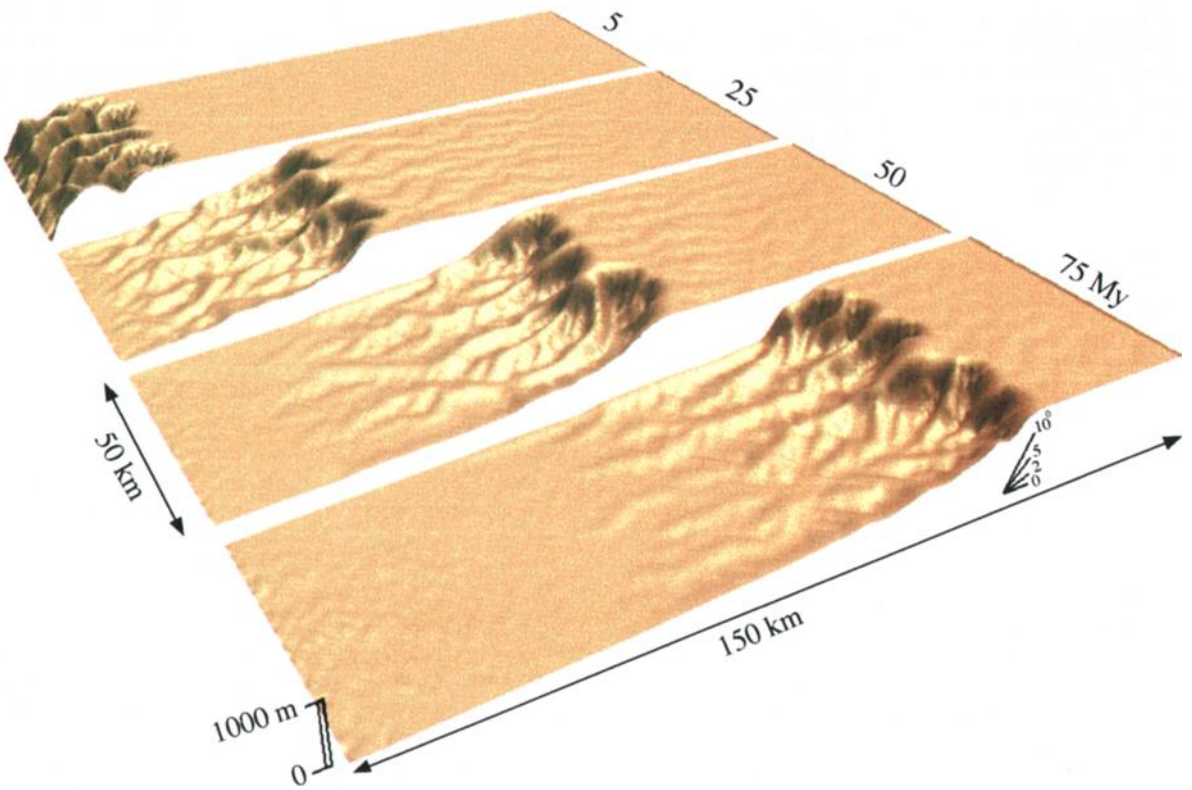

Plate 1. Planform model of escarpment evolution for a relatively arid model climate (parameter values of Table 1 and l_f=100 km for bedrock). R=50 m and grid size c_L=1 km.

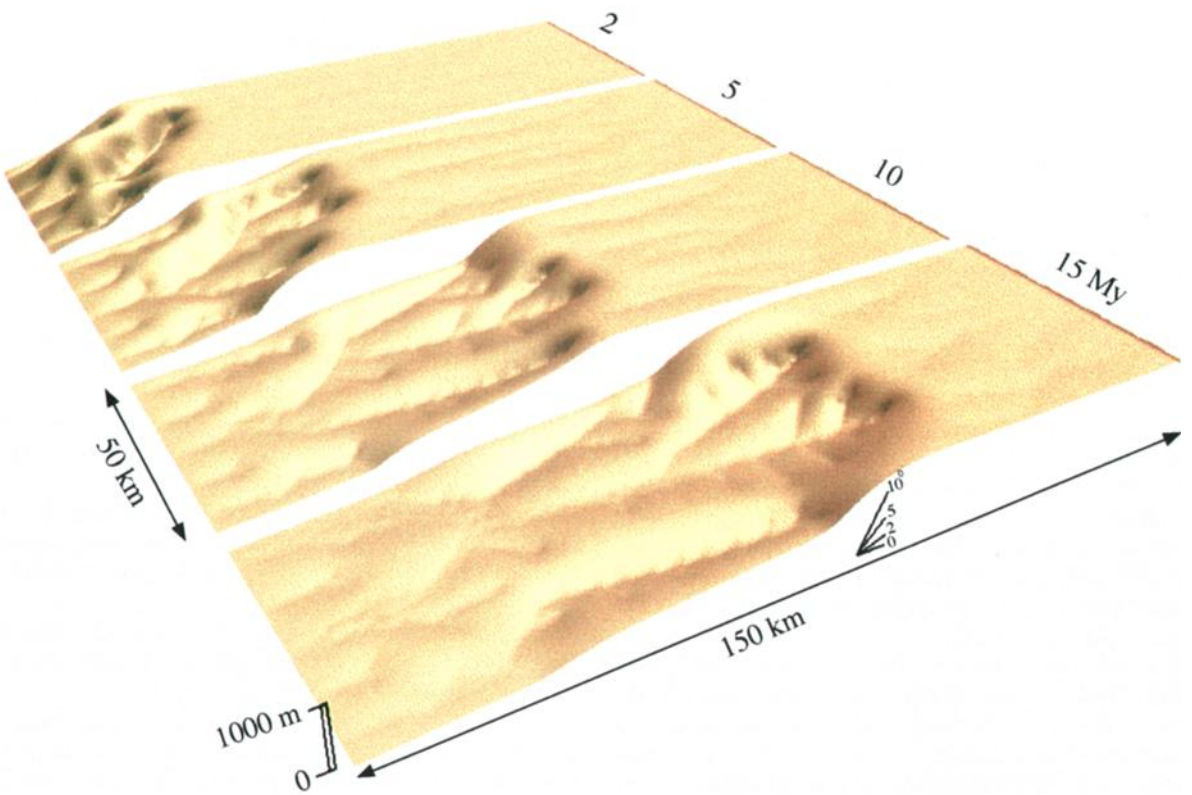

Plate 2. Planform model of scarp evolution for a relatively humid, temperate model climate (K_s and $K_f v_R$ of Table 1 multiplied by a factor of 20.0 and 1.5, respectively). R=667 m and grid size c_L=1 km.

isostatic uplift in response to denudational unloading, helps to maintain the scarp top as a divide. This is essential to preserve the escarpment gradient during retreat for a uniform lithology. Flexural isostasy also affects the scarp retreat rate.

6. When the substrate is easily eroded by fluvial processes (small reaction time/length scale of fluvial entrainment), the competition between diffusive slope decline and fluvial slope steepening is maintained only within a short distance from the divide. The escarpment retreats rapidly, decreases in height, and leaves behind an overall concave, high gradient, slowly declining, graded transport surface which may be interpreted as a pediment/pediplain.

7. When the substrate resists fluvial erosion (large reaction time/length scale and non transport-limited erosion), the competition between diffusive slope decline and fluvial slope steepening can be maintained over a long distance from the divide. The escarpment retreats slowly, maintains its height, and leaves behind a low-angle pediment/pediplain.

8. For a reaction time/length scale for fluvial entrainment of zero, which describes transport-limited erosion, fluvial erosion does not steepen slopes and there is no competition between diffusive slope decline and fluvial steepening. Escarpments decline and do not retreat.

9. For a given length scale for fluvial entrainment of bedrock, the morphology of a retreating model escarpment is determined by the ratio of the short-range diffusive and long-range advective transport efficiencies, a ratio that is interpreted to be controlled by both climate and substrate properties. A high ratio (relatively humid, temperate climate) tends to produce a low gradient convexo-concave morphology. A low ratio (relatively arid climate) promotes a steep escarpment with a sharp escarpment top and a straight main slope.

10. For a relatively arid climate steep escarpments are predicted for a wide range of escarpment heights, while for relatively humid, temperate climatic conditions, only major escarpments preserve a significant gradient.

11. When lithological contrasts are present, the models can produce complex escarpment morphologies and scarps topped with a resistant caprock form. However, a resistant caprock is not found to be an essential requirement for scarps to form and/or retreat.

Discussion

If the inferred controls on model escarpment evolution and the model behavior are to be related to natural systems, two issues must be addressed: (1) the model controls and model behavior should be compared with observations; and (2) the values and meaning of the model parameters should be related to and corroborated by those measured in other studies. The second aspect of model validation and evaluation is beyond the scope of the present paper because accurate data on processes at these scales are not available. *Gilchrist et al.* [this issue] begin to address the first issue. We show that the model behavior is consistent with the denudational history of southwestern Africa and propose styles of landscape evolution that were derived from the models and are not intuitively obvious. Here, we briefly discuss inferred model controls and behavior in relation to (1) present-day morphology of rifted margins, and (2) conceptual models of landscape evolution. Finally, we suggest how the values of the model parameters may be interpreted.

Present-Day Morphology of Rifted Continental Margins

The surface processes model predicts that erosional escarpments will only be preserved in uniform lithologies on margins that have experienced a long (>> 10 m.y.) history of denudation if the escarpment top is a drainage divide. This prediction seems to be in accord with many observations. Along large parts of the Great Escarpment of southern Africa and the margins of western India and the Red Sea, the escarpment top separates first-order drainage basins. The escarpment of east Brazil is also associated with a distinct divide [*Ollier*, 1985].

An exception is eastern Australia, where in general the escarpment top does not coincide with the major continental drainage divide which is located farther inland. However, in many segments it does coincide with a more locally defined divide. In these segments the escarpment is fairly straight with subdued embayments and promontories. In other segments, where a local divide is absent, it takes the form of deeply incised, elongated gorges [*Ollier*, 1982; *Weissel et al.*, 1992]. The latter style is consistent with planform model predictions, where under similar conditions of a distal drainage divide canyons are cut and their heads rapidly retreat toward the divide (see the companion paper [*Gilchrist et al.*, this issue]). Both observed styles are, therefore, consistent with the range of "escarpment" behavior seen in the models. The model further predicts that the areas of incised upland, without a recognizable escarpment, evolve to a clear escarpment at a drainage divide as the interfluves are removed and a lower level planation surface is created. This leads to the simple interpretation that clearly defined segments of the eastern Australian "Great Escarpment" as defined by *Ollier* [1982] correspond to places where retreat and planation to a local drainage divide has occurred. Elsewhere, the heads of the incising rivers are still seeking more inland drainage divides including the continental-scale drainage divide.

The model results predict that escarpment retreat occurs over a wide range of height scales, where diffusive processes are weak and the erosion length scale of the substrate is large. This is a "mode of landscape evolution" in the model. We interpret this result to mean that escarpments are favored by relatively arid climates and by bedrock terrains. In more humid temperate climates, where weathering rates are high, escarpments are less likely to preserve significant gradients unless an additional agent, such as vegetation, limits the diffusivity of the regolith. These predictions are at least consistent with (1) the extensive documentation of scarps and scarp retreat on various scales for semiarid to arid climatic settings [*Oberlander*, 1989; *Schmidt*, 1989] such as southwestern Africa, (2) the observation that scarps are not characteristic features where climates produce a thick regolith or saprolite, and (3) the observation that in some instances relatively humid climatic settings do have major erosional escarpments such as at the western margin of India (Figure 1).

Conceptual and Semiquantitative Models of Slope/Landscape Evolution

Comparison of the model results with conceptual models of landscape evolution may be useful because these models, although qualitative in nature, integrate a wealth of observations concerning form if not process. No universal conceptual model exists and the classical models of W.M.

Davis, W. Penck, and L.C. King are notorious for their distinctions and apparent or real controversies [e.g., *Thorn*, 1988]. The integration of conceptual models, quantitative models and observations by *Carson and Kirkby* [1972, Figures 15.7-15.9] provides a better framework for comparison. They distinguish a much greater variety of processes than the surface processes model that we use here and use threshold concepts and characteristic grain sizes of weathered material in their interpretation. Nevertheless, their predictions of slope profile development for massive sandstone, strong closely jointed rock and clay masses for both a semiarid and humid temperate climate are remarkably similar to the predictions of the surface processes model in which lithology is represented by l_f and climate by R (compare, for example, *Carson and Kirkby*'s [1972] Figure 15.7 with Figure 7 and their Figure 15.9*a* with Figure 4a). Features such as upslope convexity, main slope, and basal convexity can be recognized, and the three basic modes of main slope development, retreat, decline, and shortening are reproduced for similar climatic and lithologic conditions. Such similarities are, of course, not a true validation of either the surface processes model or the conceptual/semiquantitative model, but they do provide some confidence that the three basic processes, diffusion, reaction, and advection can replicate the larger range of complexities contemplated by *Carson and Kirkby* [1972] under the same prevailing conditions.

Model Parameter Values

We have investigated the sensitivity of the model results for a range of values of the model parameters, K_s, $K_f v_R$ and l_f, and their ratios, and for T_e. The values used are those that give styles and timescales for model evolution that are comparable to the large-scale long-term evolution of rifted continental margins. In the absence of measurements of these transport parameters at the necessary scales, the parameter values do not have any significance beyond the model. Given the lack of knowledge concerning parameter values in natural systems, the best that can be done is to make approximate estimates of the scale dependence from existing data and to show that these are consistent with the model behavior.

Diffusivity. Figure 10 shows that effective diffusivity estimates for hillslope processes from studies of fault scarp and shoreline scarp degradation increase with increasing escarpment height. It clearly demonstrates that the combined effect of the various hillslope processes is not linearly diffusive with a constant diffusivity in nature and that effective diffusivity depends on the scale at which it is measured. *Pierce and Colman* [1986] attributed the scale dependence to soil wash which transports mass at a rate which is a function of scarp size or height. Also plotted in Figure 10 are two diffusivity estimates from a theoretical modeling study of escarpment evolution by *Anderson and Humphrey* [1990] for escarpments which differ in height by more than 2 orders of magnitude. Their results are consistent with the overall trend predicted by studies of fault and shoreline scarps. We agree with *Pierce and Colman* [1986] and interpret the scale dependence to be the result of transport by surface water runoff including transport by channelized flow or fluvial transport at all scales.

The same scale dependence of effective diffusivity occurs in the numerical models, where it is related to the resolution of the model grid. It is no surprise that the K_s values found to be appropriate in this model study plot on the trend of observed diffusivities (Figure 10) at the 500-1000 m scale. This is both the scale of the model escarpments and, more importantly, the range of scales for the model grids. The explanation is that the models cannot resolve the river network when the spacing is smaller than the grid size because each model grid has only one river. Consequently, all mass transport by drainage that is more closely spaced than the grid size must be represented by diffusion and the diffusivity is scaled to achieve the necessary mass flux for slopes/relief that are smoothed at the grid scale. Diffusion in the models is therefore playing the role of both the fluvial transport at subgrid scales and true diffusion (if it exists). The same model calculated with a small grid size will resolve more of the drainage density, increase the fluvial mass transport and achieve the same large-scale model behavior with a smaller K_s value.

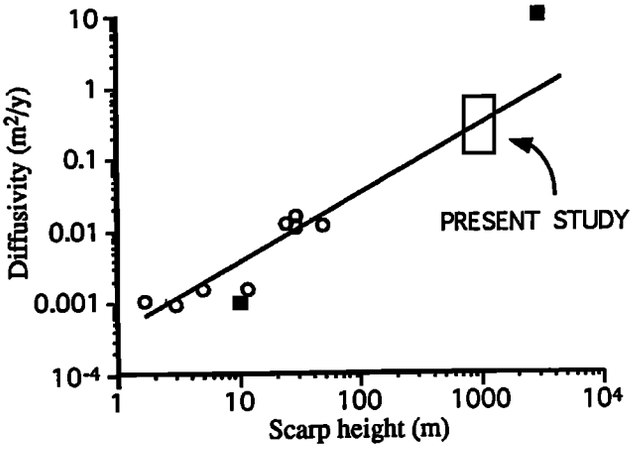

Figure 10. Plot of diffusivity estimates for hillslope transport versus escarpment height. Open circles are estimates obtained from scarp degradation studies: (1) *Hanks et al.* [1984]; (2) *Colman and Watson* [1983]; and (3) *Nash* [1980]. Solid squares are estimates from a theoretical modeling study of escarpment evolution by *Anderson and Humphrey* [1990]. The open rectangle corresponds to the range of values of K_s required to produce retreat of an ~1-km-high escarpment in the present study.

The importance of both the model and observed scale dependence of the effective diffusivity is that they both provide the same scale-dependent information as a surrogate for the real processes. If degradation is measured in the field on a 1000-m-high scarp at a 1000-m scale and fitted to a diffusive model, the effective diffusivity will plot on the trend line of Figure 10 and will agree with the diffusivities used in numerical models with a 1000-m grid size. If this interpretation is correct, measured and model effective diffusivities can be compared, provided that the scale dependence is acknowledged and the comparison is made for estimates made at the same scale.

Erosion length scale and fluvial transport coefficient. Similarly, it is not obvious how to make a useful comparison between the numerical values of l_f and K_f and related empirical or physical parameter values determined by short time-scale and small spatial scale measurements. For example, as demonstrated in the appendix, K_f may contain information on the magnitude-frequency distribution of

discharge events. Moreover, K_f probably also depends on the dominant river type and grain size distribution [*Paola and Heller*, 1992]. l_f likely depends not only on the cohesive strength of the substrate or detachability but also on the abrasive power of the fluvial system, that is, on the characteristics of the sediment load that is being advected. Both K_f and l_f are lumped parameters, like thermodynamic parameters, which reflect the combination of many processes which scale with space and time. When l_f and K_f estimates are available from field measurements for the scales appropriate to the models, a comparison and understanding of the behavior, like that for K_s, may be achieved.

Appendix: Rationale for a Linear Capacity for the Model Rivers

Several model studies [e.g., *Kirkby*, 1986; *Willgoose et al.*, 1991b] employ a nonlinear sediment transport relationship for carrying capacity

$$q_f^{eqb} = -C_f (q_r)^n S^m \tag{A1}$$

where q_r is river discharge per unit with, S is local slope, and C_f is a transport coefficient. This general relationship has been widely used in empirical [see *Carson and Kirkby*, 1972] studies of sediment transport on short timescales. It can be derived using the common assumption that sediment transport is a function of bottom channel shear stress τ [*Gessler*, 1971; *Vanoni*, 1975; *Willgoose et al.*, 1991b; *Paola and Heller*, 1992]

$$q_f = C_1 (\tau - \tau_c)^p \tag{A2}$$

where C_1 and p are empirical constants and τ_c is the critical bottom shear stress below which no entrainment occurs (it is generally assumed that $\tau >> \tau_c$).

We use the simple linear form of (A1), with n=m=1, in this paper (equation (4)) for a number of reasons. First, no agreement exists on the powers n and m. Commonly used values of p range from 3/2 [*Begin et al.*, 1981; *Paola and Heller*, 1992] to 3 [e.g., *Willgoose et al.*, 1991b], leading to values of n and m in the range of 1 to 2. *Leopold et al.* [1964] suggested n=5/2 and *Kirkby* [1986] employed n=3. We therefore first want to understand how interactions occur in a linear system. Second, for the scales of interest in this study the resolution c_L does not reproduce local high slopes where a nonlinear slope dependence would be most important. Third, it is shown below that even when a nonlinear discharge dependence is appropriate for fluvial transport on short timescales, a linear discharge dependence is appropriate for long timescales provided that the model time steps Δt are greater than the recurrence time of the maximum size flood and that slopes are not significantly altered by erosion on time scales less than Δt.

When $n > 1$, as suggested in most studies, knowledge of the magnitude-frequency distribution of discharge is important to assess the long-term averaged carrying capacity; a small number of large events (stormy climate) transports more effectively than a large number of small events if they represent the same long-term averaged amount of discharge.

Let the magnitude-frequency distribution of discharge for a given location in a drainage basin be described as the probability P of occurrence of discharge of magnitude q_r

$$P = f(q_r) \tag{A3}$$

where f is an arbitrary function. Further assume that the size of possible discharge occurrences ranges between q_r^{min} and q_r^{max}. In general, P decreases with increasing q_r and q_r^{max} corresponds to the rare, extreme flood event which has a high recurrence interval t^{max} [e.g., *Leopold et al.*, 1964].

An estimate of the average discharge over a time interval Δt is given by

$$< q_r > = \frac{\Delta t}{t^{max}} \int_{q_r^{min}}^{q_r^{max}} f(q_r) dq_r . \tag{A4}$$

When $\Delta t >> t^{max}$ this estimate is very accurate and $< q_r > = C_2$, where C_2 is a constant. Similarly, an estimate of the average carrying capacity can be obtained by integrating (A1). When changes in local slope S can be ignored during Δt one obtains.

$$< q_f^{eqb} > = \frac{\Delta t}{t^{max}} \int_{q_r^{min}}^{q_r^{max}} f(q_r) d(C_f q_r^n S^m) = C_f S^m \frac{\Delta t}{t^{max}} \int_{q_r^{min}}^{q_r^{max}} f(q_r) q_r^{n-1} dq_r \tag{A5}$$

When $\Delta t >> t^{max}$, this estimate is also very accurate and $< q_f^{eqb} > = C_f S^m C_3$, where C_3 is a constant. It follows that

$$< q_f^{eqb} > = C_4 C_f < q_r > S^m \tag{A6}$$

where $C_4 = C_3/C_2$ is a constant. C_4 contains information on the magnitude-frequency distribution of discharge.

Equation (A6) demonstrates that the nonlinear dependence of carrying capacity on discharge in (A1) is lost on long timescales when the model time steps Δt are greater than the recurrence time t^{max} of the maximum size flood and slopes are not significantly altered by erosion on timescales $< \Delta t$. When these conditions are satisfied, information about the temporal magnitude-frequency distribution of discharge (or storminess of climate) is, on long timescales, represented by an effective nondimensional fluvial transport coefficient, $k_f = C_f C_4$, in the carrying capacity relationship. This suggests that the transport coefficient is complex because it contains information on climate and, consequently, that its numerical value cannot be simply compared with transport coefficients appropriate for short timescales.

Acknowledgments. This work was funded by an NSERC operating grant to C.B. and during much of this work, H.K. was supported by a Dalhousie University Killam Postdoctoral Fellowship. The work benefitted from many constructive discussions with Philippe Fullsack, Alan Gilchrist, and Susan Ellis. Susan Ellis compiled the data for Figure 10 and provided constructive comments on the manuscript. Rudy Slingerland and Mike Ellis are thanked for their thorough and constructive reviews. Support for reproduction of color plates has been provided by NASA Grant NAGW 3338 to Michael A. Ellis.

References

Ahnert, F., Brief description of a comprehensive three-dimensional process-response model for landform development, *Z. Geomorphol., Suppl., 25*, 29-49, 1976.

Ahnert, F., Process-response models of denudation at different spatial scales, *Catena Suppl., 10*, 31-50, Catena Verlag, 1987.

Anderson, R.S., and N.F. Humphrey, Interaction of weathering and transport processes in the evolution of arid landscapes, in *Quantitative Dynamic Stratigraphy*, edited by T.A. Cross, pp. 349-361, Prentice-Hall, Englewood Cliffs, N.J., 1990.

Andrews, D.J., and R.G. Bucknam, Fitting degradation of

shoreline scarps by a nonlinear diffusion model, *J. Geophys. Res., 92,* 12,857-12,867, 1987.

Armstrong, A.C., A three-dimensional simulation of slope forms, *Z. Geomorphol., Suppl., 25,* 20-28, 1976.

Armstrong, A.C., Soils and slopes in a humid environment, *Catena, 7,* 327-338, 1980.

Beaumont, C., P. Fullsack, and J. Hamilton, Erosional control of active compressional orogens, in *Thrust Tectonics,* edited by K.R. McClay, pp. 1-18, Chapman and Hall, London, 1992.

Begin, Z.B., ERFUS 6-A FORTRAN program for calculating the response of alluvial channels to baselevel lowering, *Comput. Geosci., 13,* 389-398, 1987.

Begin, Z.B., D.F. Meyer, and S.A. Schumm, Development of longitudinal profiles of alluvial channels in response to base-level lowering, *Earth. Surf. Processes Landforms, 6,* 49-68, 1981.

Beven, K.J., and M.J. Kirkby, A physically-based variable contributing area model of basin hydrology, *Hydrol. Sci. J., 24,* 43-69, 1979.

Bohannon, R.G., C.N. Naeser, D.L. Schmidt, and R.A. Zimmermann, The timing and uplift, volcanism, and rifting peripheral to the Red Sea: A case for passive rifting?, *J. Geophys. Res., 94,* 1683-1701, 1989.

Brown, R.W., D.J. Rust, M.A. Summerfield, A.J.W. Gleadow, and M.C.J. De Wit, An Early Cretaceous phase of accelerated erosion on the south-western margin of Africa: Evidence from apatite fission track analysis and the offshore sedimentary record, *Nucl. Tracks Radiat. Meas., 17,* 339-350, 1990.

Carson, M.A., and M.J. Kirkby, *Hillslope Form and Process,* 475 pp., Cambridge University Press, New York, 1972.

Chase, C.G., Fluvial landsculpting and the fractal dimension of topography, *Eos Trans. AGU, 69,* 1207, 1988.

Chase, C.G., Fluvial landsculpting and the fractal dimension of topography, *Geomorphology, 5,* 39-57, 1992.

Colman, S.M., and K. Watson, Ages estimated from a diffusion equation model for scarp degradation, *Science, 221,* 263-265, 1983.

Cordova, J.R., I. Rodriguez-Iturbe, and P. Vaca, On the development of drainage networks, recent developments in the explanation and prediction of erosion and sediment yield, *IASH Publ., 137,* 239-249, 1983.

Culling, W.E.H., Analytical theory of erosion, *J. Geol., 68,* 336-344, 1960.

Culling, W.E.H., Theory of erosion of soil-covered slopes, *J. Geol., 73,* 230-254, 1965.

Dietrich, W.E., C.J. Wilson, D.R. Montgomery, and J.M. Romy Bauer, Erosion thresholds and land surface morphology, *Geology, 20,* 675-679, 1992.

Gardner, T.W., Experimental study of knickpoints and longitudinal profile evolution in cohesive, homogeneous material, *Geol. Soc. Am. Bull., 94,* 664-672, 1983.

Gessler, J., Aggradation and degradation, in *River Mechanics,* edited by H.W. Shen, pp. 8.1-8.24, Water Res. Publ., Fort Collins, Colo., 1971.

Gilbert, G.K., *Report on the Geology of the Henry Mountains,* 160 pp., U.S. Geological Survey Rocky Mountain Region, Washington, D.C., 1877.

Gilchrist, A.R., and M.A. Summerfield, Differential denudation and flexural isostasy in formation of rifted-margin upwarps, *Nature, 346,* 739-742, 1990.

Gilchrist, A.R., H. Kooi, and C. Beaumont, The post-Gondwana geomorphic evolution of south-western Africa: Implications for the controls on landscape development from observations and numericl experiments, *J. Geophys. Res.,* this issue.

Hanks, T.C., R.C. Bucknam, K.R. Lajoie, and R.E. Wallace, Modification of wave-cut and faulting-controlled landforms, *J. Geophys. Res., 89,* 5771-5790, 1984.

Hirano, M., A mathematical model of slope development, *J. Geosci. Osaka, 11,* 13-52, 1968.

Horton, R.E., Erosional development of streams and their drainage basins; hydrophysical approach to quantitative morphology, *Geol. Soc. Am. Bull., 56,* 275-370, 1945.

Howard, A.D., Thresholds in river regimes, in *Thresholds in Geomorphology,* edited by D.R. Coates and J.D. Vitek, Allen and Unwin, Boston, Mass., 1980.

Howard, A.D., and G. Kerby, Channel changes in badlands, *Geol. Soc. Am. Bull., 94,* 739-752, 1983.

Johnson, D.D., and C. Beaumont, Preliminary results from a planform kinematic model of orogen evolution, surface processes and the development of clastic foreland basin stratigraphy, *Spec. Publ. Soc. Econ. Paleontol. Mineral.,* in press, 1994.

King, L.C., Canons of landscape evolution, *Geol. Soc. Am. Bull., 64,* 721-753, 1953.

King, L.C., Pediplanation and isostasy: an example from South Africa, *Q. J. Geol. Soc., 111,* 353-359, 1955.

King, L.C., *Wandering Continents and Spreading Sea Floors on an Explanding Earth,* 232 pp., John Wiley, New York, 1983.

Kirkby, M.J., Hillslope process-response models based on the continuity equation, in Slope Form and Process, edited by D. Brunsden, *Inst. Br. Geogr. Spec. Publ., 3,* 15-30, 1971.

Kirkby, M.J., A two-dimensional simulation model for slope and stream evolution, in *Hillslope Processes,* edited by A.D. Abrahams, pp. 203-222, Allen and Unwin, Boston, Mass., 1986.

Leopold, L.B., and W.B. Langbein, The concept of entropy in landscape evolution, *U.S. Geol. Surv. Prof. Pap., 500-A,* 1962.

Leopold, L.B., M.G. Wolman, and J.P. Miller, *Fluvial Processes in Geomorphology,* 522 pp., Freeman, New York, 1964.

Mackin, J.H., Concept of the graded river, *Geol. Soc. Am. Bull., 59,* 463-512, 1948.

Moore, M.E., A.J.W. Gleadow, and J.F. Lovering, Thermal evolution of rifted continental margins: New evidence from fission tracks in basement apatites from south-eastern Australia, *Earth Planet. Sci. Lett., 87,* 255-270, 1986.

Morisawa, M., *Rivers, Form and Process,* 222 pp., Longman, London, 1985.

Nash, D.B., Forms of bluffs degraded for different length of time in Emmet County, Michigan, U.S.A., *Earth Surf. Processes., 5,* 331-345, 1980.

Oberlander, T.M., Slope and pediment systems, in *Arid Zone Geomorphology,* edited by D.S.G. Thomas, pp. 56-84, Belhaven, London, 1989.

Ollier, C.D., The Great Escarpment of eastern Australia: tectonic and geomorphic significance, *J. Geol. Soc. Aust., 29,* 13-13, 1982.

Ollier, C.D., Morphotectonics of continental margins with great escarpments, in *Tectonic Geomorphology,*

Binghamton Symp. Geomorphol. Int. Ser., vol. 15, edited by M. Morisawa and J.T. Hack, pp. 3-25, Allen and Unwin, Boston, Mass., 1985.

Partridge, T.C., and R.R. Maud, Geomorphic evolution of southern Africa since the Mesozoic, *S. Afr. J. Geol., 90,* 179-208, 1987.

Paola, C., and P.L. Heller, The large-scale dynamics of grain-size variation in alluvial basins, 1, Theory, *Basin Res., 4,* 73-90, 1992.

Pierce, K.L., and S.M. Colman, Effect of height and orientation (microclimate) on geomorphic degradation rates and processes, late-glacial terrace scarps in central Idaho, *Geol. Soc. Am. Bull., 97,* 869-885, 1986.

Schmidt, K.H., The significance of scarp retreat for Cenozoic landform evolution on the Colorado Plateau, U.S.A., *Earth Surf. Processes Landforms, 14,* 93-105, 1989.

Schumm, S.A., *The Fluvial System,* 338 pp., John Wiley, New York, 1977.

Seidl, M.A., and W.E. Dietrich, The problem of channel erosion into bedrock, *Catena Suppl., 23,* 101-1024, 1992.

Shaw, G.H., and H.D. Mooers, Development of drainage networks: a numerical model, *Eos Trans. AGU, 69,* 362, 1988.

Smith, T.R., and F.P. Bretherton, Stability and the conservation of mass in drainage basin evolution, *Water Resour. Res., 8,* 1506-1529, 1972.

Sprunt, B., Digital simulation of drainage basin development, in *Spatial Analysis in Geomorphology,* edited by R.J. Chorley, pp. 371-389, Methuen, New York, 1972.

Summerfield, M.A., *Global Geomorphology,* 537 pp., John Wiley, New York, 1991.

Thorn, C.E., *Introduction to Theoretical Geomorphology,* 247 pp., Unwin and Hyman, Boston, Mass., 1988.

Vanoni, V.A., *Sedimentation Engineering,* American Society of Civil Engineers, New York, 1975.

Weissel, J.K., G.D. Karner, and A. Malinverno, Tectonics and erosion: topographic evolution of rift flanks and rifted continental margins, paper presented at Chapman Conference on Tectonics and Topography, AGU, Snowbird, Utah, 1992.

Willgoose, G., R.L. Bras, and I. Rodriguez-Iturbe, Results from a new model of river basin evolution, *Earth Surf. Processes Landforms, 16,* 237-254, 1991a.

Willgoose, G., R.L. Bras, and I. Rodriguez-Iturbe, A coupled channel network growth and hillslope evolution model, 1, Theory, *Water Resour. Res., 27,* 1671-1684, 1991b.

Wood, E.F., M. Sivapalan, and K. Beven, Similarity and scale in catchment storm response, *Rev. Geophys., 28,* 1-18, 1990.

H. Kooi and C. Beaumont, Department of Oceanography, Dalhousie University, Halifax, Nova Scotia, Canada B3H 4J1.

(Received March 30, 1993; revised October 15, 1993; accepted December 28, 1993.)